Characterization of molecular and cellular mechanisms regulating NLRP3 inflammasome activity

Andrey A Shuvarikov

A dissertation

submitted in partial fulfillment of the

requirements for the degree of

Doctor of Philosophy

University of Washington

2021

Reading Committee:

Michael Gale, Jr., Chair

Adam Geballe

Andrew Oberst

Program Authorized to Offer Degree:

Molecular and Cellular Biology

University of Washington

Abstract

Characterization of molecular and cellular mechanisms regulating NLRP3 inflammasome activity

Andrey A Shuvarikov

Chair of the Supervisory Committee:

Michael Gale, Jr.

Department of Immunology

The NLRP3 protein is a key initiator of inflammation in humans. NLRP3 becomes activated by a multitude of danger signals, including microbial infection, metabolic dysfunction, and cell-internalized particulates. Upon activation, NLRP3 nucleates formation of a multiprotein complex called the inflammasome, in which caspase-1 activity mediates processing of the pro-inflammatory cytokines IL-1β and IL-18 and induces pyroptosis, a pro-inflammatory form of cell death. While multiple regulators of the NLRP3 inflammasome have been described, specific ligands of NLRP3 and a comprehensive mechanism for its activation remain largely unknown. We performed a proteomics screen using co-immunoprecipitation (IP) and mass spectrometry to identify cellular proteins that bind NLRP3. Using this screen, we identified multiple NLRP3 interactors, including a family of mitochondrial solute carrier proteins. Co-IP experiments verified that four of these carriers, namely CTP, ANT3, OGC, and Citrin, specifically interact with NLRP3. Because of its linkage with metabolic and inflammatory diseases, we further assessed the role of Citrin, a calcium-binding aspartate/glutamate carrier, in inflammasome

function. When overexpressed, Citrin induced IL-1β release and inflammasome nucleation, while CRISPR/Cas9 knockout of Citrin from THP-1 macrophages significantly abrogated NLRP3-dependent pyroptosis, IL-1β release, and ASC speck formation. Citrin's ability to promote NLRP3 inflammasome activation was dependent on its calcium-sensing N-terminal domain. Importantly, Citrin's regulatory function was specific to NLRP3 and did not affect the AIM2 inflammasome or other cell death pathways. Altogether, our studies identify Citrin as a new mitochondrial regulator of the NLRP3 inflammasome.

Acknowledgements

As I complete my PhD studies, I am grateful to the many mentors and colleagues who helped me on this path. To begin, I would like to thank all members of the Gale lab, both past and present, with whom I had the pleasure of working during the past several years. The Gale lab is composed of friendly, collaborative, and hard-working professionals who made the work atmosphere both enjoyable and motivating. Particularly, I would like to thank Michael Davis for his mentorship and support, and for ultimately directing my attention to a family of proteins that became the focus of my thesis project. Many thanks also to Katharina Esser-Nobis for her expertise and work on fractionation experiments. I am also grateful to Justin Roby, Alison Kell, Lauren Hatfield, Kathryn McGuckin Wuertz, Rebecca Olson, Nick Hubbard, Leanne Whitmore, Connor Driscoll, Richard Green, Sean White, Kathleen Voss, Olivia Kern, Brian Turnbull, Tien-Ying Hsiang, Amina Negash, Marian Fairgrieve, Dan Newhouse, Jean Chang, and Jenny Go for their advice, support, and help with experiments. A special thanks to Elyse Verstelle, Jackie Berhorst, and Nanette Crochet, without whom our lab would never run smoothly. I am very grateful to my wife, Evelina, and our children, Andrey, Rebecca, and Mariana, for their patience, understanding, and support during my doctoral studies. Many thanks also to our parents and extended family, who were always encouraging and supportive, especially during difficult times. I am grateful for the funding and administrative support provided by the UW Molecular and Cellular Biology PhD program and Immunology Department, as well as the funding sources that supported my work (NSF GRFP Grant DGE-1256082; NIH grants R01 AI118916, R01 AI104002, and R01 AI127463). Finally, I would like to extend a special thank you to my PI, Dr. Michael Gale, Jr., as well as members of my supervisory committee, Dr. Michael Emerman, Dr. Adam Geballe, Dr. Michael Lagunoff, and Dr. Andrew Oberst, for their mentorship and guidance.

Table of Contents

List of Figures

List of Tables

1. Introduction

1.1. Inflammation and Immunity

Inflammation is an important and powerful weapon in the human body's arsenal of immune defenses against both pathogenic and non-pathogenic threats. When deployed properly, inflammation can be protective by facilitating pathogen clearance and tissue repair. However, when inflammation becomes dysregulated, this can lead to many detrimental health consequences, including chronic inflammatory disorders, tissue damage, and even death. For this reason, the human body employs numerous molecular and cellular mechanisms to keep inflammation under strict, regulatory control.

Inflammation is initiated when the body encounters external or internal agents that threaten tissue homeostasis. Such threats include microbes, toxins, irritants, particulates, as well as markers of tissue damage or metabolic dysfunction. Many of these stimuli are detected by innate immune sensor proteins called pattern recognition receptors (PRRs), which recognize specific molecular motifs, such as pathogen-associated molecular patterns (PAMPs) or damage-associated molecular patterns (DAMPs). Upon recognition of a PAMP or DAMP, PRRs trigger intracellular signaling pathways that culminate in release of pro-inflammatory mediators. These mediators include cytokines and chemokines, which activate the endothelium of proximal blood vessels, facilitate migration of neutrophils and other leukocytes to the affected tissue, and also activate leukocytes for mediation of immune responses (Medzhitov 2008; Dinarello 2009). Once leukocytes arrive at the site of infection or damage, they become activated and initiate the process of pathogen elimination or removal of a sterile threat. If the threat is successfully eliminated, inflammation transitions into its resolution phase, whereby recruited monocytes and macrophages remove dead cells and begin rebuilding damaged tissue. In the event that a threat persists and cannot be

sufficiently removed, a state of chronic inflammation ensues. Chronic inflammation serves as the underlying cause of many human diseases, including Type 2 diabetes, Alzheimer's, and atherosclerosis (Strowig et al., 2012). From this we see that inflammation is a powerful physiological response that helps protect the body from agents that threaten its health and survival, yet it can also be the cause of serious illness when its activation goes unchecked. Fortunately, multiple regulatory mechanisms exist within cells and tissues to ensure that inflammation is deployed in the proper physiological context.

1.2. The Inflammasomes

One key molecular pathway by which inflammation is regulated involves the activity of multiprotein complexes called the inflammasomes. Inflammasomes generally consist of three major components: a sensor PRR protein that responds to specific intracellular threats, the adaptor protein ASC (apoptosis-associated speck-like protein with a caspase recruitment domain (CARD)), and an effector cysteine protease called caspase-1 (Schroder and Tschopp, 2010; Sutterwala et al., 2014). Each inflammasome PRR undergoes activation in response to a specific ligand or set of stimuli. To date, five inflammasome sensors have been well-characterized in humans. These include pyrin, AIM2 (absent in melanoma 2), NLRC4 (nucleotide-binding domain leucine-rich repeat and CARD containing receptor 4), NLRP1 (NLR and pyrin domain containing receptor 1), and NLRP3. Pyrin senses pathogen-induced downregulation of RhoA GTPase activity, which triggers its activation and subsequent inflammasome assembly (Schnappauf et al., 2019). AIM2 surveils the cell for cytosolic double-stranded (ds)DNA, which binds directly to its HIN-200 domain and induces AIM2 activation (Rathinam et al., 2010). NLRC4 does not bind its ligands directly; rather, flagellin or needle protein from Type 3 secretion systems of Gram-negative bacteria bind to NAIP (neuronal apoptosis inhibitor protein), which then associates with NLRC4

to nucleate the inflammasome (Zhao et al., 2011; Yang et al., 2013). Human NLRP1 becomes activated by enteroviruses through a functional degradation mechanism, in which enteroviral 3C protease cleaves the autoinhibitory N-terminal domain of NLRP1, thereby liberating the NLRP1 C-terminal domain and enabling it to nucleate the inflammasome complex (Sandstrom et al., 2019; Robinson et al., 2020). NLRP3, meanwhile, can be activated by a wide range of stimuli, including PAMPs, DAMPs, toxins, and internalized particulates (Lamkanfi et al., 2012; Swanson et al., 2019). The chemical diversity of these stimuli suggests a mechanism in which NLPR3 does not bind all ligands directly, but instead senses common intracellular changes that all of these stimuli induce.

Once activated, inflammasome sensors self-oligomerize and nucleate the inflammasome complex by recruiting ASC through PYD-PYD interactions. ASC then self-oligomerizes to form ASC filaments, which serve as a platform for recruitment of pro-caspase-1 through CARD-CARD interactions with ASC (Sutterwala et al., 2014). The resulting inflammasome complex appears as an "ASC speck" when viewed by microscopy. Once it is recruited to the inflammasome complex, pro-caspase-1 cleaves itself at the linker between its C-terminal p10 and central p20 domains, thereby activating its proteolytic p10 subunit (Boucher et al., 2018). Activated caspase-1 then proceeds to cleave multiple intracellular targets, including pro-interleukin (IL)-1β and pro-IL-18, inflammatory cytokines which are cleaved into their active, secreted forms. Caspase-1 activity also leads to pyroptosis, a pro-inflammatory form of cell death that facilitates release of IL-1β and IL-18, as well as other inflammatory molecules, into the extracellular space, where they exert inflammatory effects on surrounding cells and tissues. Through these signaling pathways, the inflammasomes serve as initiators and critical regulators of inflammation at a molecular level. While activation mechanisms for pyrin, AIM2, NLRP1, and NLRC4 inflammasomes have been

well-defined, the precise mechanism for NLRP3 inflammasome activation remains a mystery. Given the importance of NLRP3 in multiple human diseases and immune responses to pathogens (reviewed in Kanneganti et al., 2010; Strowig et al., 2012; Lupfer et al., 2015), countless studies have sought to characterize its signaling pathway. As a result, significant advancements have been achieved in our understanding of NLRP3 inflammasome regulation, though, as of this writing, a comprehensive and unifying mechanism of NLRP3 activation remains elusive.

1.3. Mechanisms Regulating NLRP3 Inflammasome Activity

1.3.1. NLRP3: A Unique Sensor

NLRP3 (also known as NALP3 or cryopyrin) is a 118 kilodalton (kD) protein consisting of an N-terminal PYD (pyrin) domain, a central NACHT domain (so named because it is found in NAIP, CIITA, HET-E, and TEP1 proteins), and a C-terminal LRR (leucine-rich repeat) domain (Swanson et al., 2019). The NLRP3 PYD domain interacts with ASC to initiate inflammasome complex formation, while the LRR domain mediates interactions with other key binding partners and regulators of NLRP3. The NACHT domain exhibits ATPase activity, a function which is essential for NLRP3 activation and self-oligomerization (Duncan et al., 2007). Upon activation, NLRP3 self-associates to form a molecular platform, which then nucleates formation of an inflammasome complex through recruitment of ASC and procaspase-1. In addition to ASC and caspase-1, the NLRP3 inflammasome also requires NEK7 (never in mitosis A-related kinase 7) for its activation and function (Shi et al., 2015; He et al., 2016). NEK7 is a serine/threonine kinase that associates directly with NLRP3, but not with NLRC4 or AIM2 (Shi et al., 2015). Recent structural studies using cryo-electron microscopy uncovered that the NEK7 C-terminal domain binds NLRP3 LRR and NACHT domains, which may serve to bridge adjacent NLRP3 molecules to enable formation of the NLRP3 inflammasome nucleation platform (Sharif et al., 2019). Apart

from its inflammasome function, NLRP3 has also been reported to act as a transcription factor promoting T helper Type 2 cell differentiation (Bruchard et al., 2015) and to promote hypoxia-induced mitochondrial ROS (reactive oxygen species) production in renal cells (Kim et al., 2018). Though many different cell types express the NLRP3 protein, functional NLRP3 inflammasome signaling machinery is predominantly harbored by certain barrier cells, such as keratinocytes, as well as immune cells, including macrophages, dendritic cells, and monocytes. In what follows, we review what is currently known about molecular regulation of the NLRP3 inflammasome and identify gaps in our understanding of this complex biological pathway.

1.3.2. Signal 1 – Priming

To begin, in almost all cases, the NLRP3 inflammasome requires two signals for its activation. This requirement adds an additional layer of control to the NLRP3 inflammasome pathway, helping to prevent its aberrant activation and underscoring the importance of strictly regulating inflammation at a molecular level. The purpose of the first signal is to prepare, or license, the cell for inflammasome complex formation. This priming is achieved, first and foremost, through transcriptional upregulation of NLRP3 and proIL-1β (Sutterwala et al., 2014). Pro-IL-1β is typically not expressed in resting macrophages, while NLRP3 is expressed at low levels. Procaspase-1, ASC, and proIL-18, meanwhile, are constitutively expressed and generally do not require upregulation for inflammasome activity. Priming can be initiated by many different signals, all of which relay a context of danger within or outside the cell. These priming signals include PAMPs such as LPS (lipopolysaccharide) or MDP (muramyl dipeptide), which engage PRRs like TLR (toll-like receptor) proteins or NOD2 (nucleotide-binding oligomerization domain-containing protein 2) (Bauernfeind et al., 2009). Alternatively, priming can be induced by cytokines, such as TNFα (tumor necrosis factor α) or IL-1β, following their engagement of IL-1

or TNF receptors (Franchi et al., 2009). Ultimately, all these priming signals trigger a signaling cascade that culminates in activation of the transcription factor, NF-κB (nuclear factor-κB), which promotes transcription of pro-IL-1β, NLRP3, and other inflammatory mediators (Bauernfeind et al., 2009; He et al, 2016) (**Figure 1.1**). LPS priming also evokes metabolic changes in macrophages, causing them to undergo a shift from oxidative phosphorylation to glycolysis, which results in accumulation of succinate (Tannahill et al., 2013). Succinate, in turn, stabilizes HIF1α (hypoxia-inducible factor 1-α), leading to increased proIL-1β transcription (Tannahill et al., 2013). In addition to transcriptional regulation, inflammasome priming also induces subcellular relocation of NLRP3 inflammasome components and post-translational modifications to NLRP3, events which will be addressed in a later section.

1.3.3. Signal 2 - Activation

Once a cell is licensed for NLRP3 activation by signal one, it is effectively primed and on standby, awaiting a second signal to activate NLRP3 and trigger formation of the inflammasome complex. Unlike most PRRs, which respond to a narrow range of stimuli, NLRP3 possesses the remarkable ability to respond to a wide assortment of activating signals (**Figure 1.1**). These activators of NLRP3 include microbial infection; toxins such as nigericin or streptolysin O; endogenous DAMPs including extracellular ATP, monosodium urate (MSU) crystals, or amyloid-β; exogenous particulates like alum or silica; and markers of metabolic dysfunction such as oxidized mitochondrial DNA (ox-mtDNA) or cytosolic hexokinase (Mariathasan et al., 2006; Martinon et al., 2006; Dostert et al., 2008; Hornung et al., 2008; Halle et al., 2008; Harder et al., 2009; Schroder and Tschopp, 2010; Misawa et al., 2013; Wolf et al., 2016). Because these activators are so chemically different, it is highly improbable that all of them function as direct ligands of NLRP3. It is therefore generally accepted that all or most NLRP3 stimuli converge in

their ability to induce common cellular stress signals, which work either together or apart to activate NLRP3. These cell stress signals include ionic flux, lysosomal rupture, mitochondrial dysfunction, and Golgi disruption, cellular perturbations which will be discussed in the foregoing sections.

1.3.3.1. Cellular Ionic Flux

Intracellular ionic concentrations are strictly regulated to maintain homeostatic function of cellular processes, membranes, and proteins. Sudden and significant changes to these ionic concentrations can therefore serve as a signal of intracellular damage that is directly or indirectly sensed by NLRP3, thereby triggering its activation. Indeed, one common cellular perturbation evoked by virtually all NLRP3 stimuli is potassium ion (K^+) efflux. Numerous NLRP3 stimuli, including nigericin (a K^+/H^+ ionophore), extracellular ATP, or crystalline particulates like MSU induce K^+ efflux from the cell either through pore formation or activation of K^+ channels in the plasma membrane (Muñoz-Planillo et al., 2013; Di et al., 2018). In a study performed by Petrilli and colleagues, K^+ efflux was shown to be a necessary upstream signal for NLRP3 inflammasome activation, since high extracellular K^+ concentrations inhibited NLRP3 activation in macrophages, while low K^+ concentration in macrophage lysates triggered NLRP3 inflammasome assembly (Petrilli et al., 2007). However, certain stimuli, such as the drugs imiquimod and CL097, along with the mitochondrial protein hexokinase, induce NLRP3 inflammasome activity independently of K^+ efflux, challenging the notion that K^+ efflux is the only cellular stress signal driving NLRP3 activation (Groβ et al., 2016; Wolf et al., 2016).

In addition to K^+ efflux, intracellular Ca^{2+} mobilization has also been implicated in regulation of the NLRP3 inflammasome. A critical regulator of Ca^{2+} signaling and mobilization is a protein called phospholipase C (PLC). When activated, PLC cleaves PIP_2 (phosphatidylinositol

4,5-bisphosphate) into IP_3 (inositol 1,4,5-trisphosphate) and DAG (diacylglycerol). IP_3 then binds to IP_3R (IP_3 receptor), an ER-localized calcium channel, which releases ER Ca^{2+} stores into the cytoplasm. Multiple NLRP3 stimuli promote Ca^{2+} influx into the cytosol; prevention of this Ca^{2+} influx through knockdown or inhibition of IP_3R was shown to inhibit NLRP3 inflammasome activation (Lee et al., 2012; Murakami et al., 2012). Activation of the calcium-sensing receptor (CASR) on the plasma membrane was also demonstrated to induce NLRP3 activation through the activity of PLC (Lee et al., 2012). The precise mechanism by which Ca^{2+} influx regulates NLRP3 activation, however, remains unclear. It is possible that Ca^{2+} simply functions as a counterion to balance the loss of K^+. Alternatively, Ca^{2+} movement from ER stores into mitochondria may induce mitochondrial dysfunction, which then triggers NLRP3 inflammasome activation (Murakami et al., 2012; Horng 2014). At least one study showed that Ca^{2+} mobilization was neither necessary nor sufficient for NLRP3 activation by nigericin or ATP, which signal through K^+ efflux (Katsnelson et al., 2015). More investigations are needed, therefore, to understand the precise role of Ca^{2+} mobilization in NLRP3 regulation.

1.3.3.2. Lysosomal Disruption

Another proposed activating signal for NLRP3 is lysosomal disruption. When macrophages phagocytose particulate stimuli that activate NLRP3, such as MSU, silica, cholesterol crystals, or alum, this leads to lysosomal rupture and release of lysosomal proteases called cathepsins into the cytoplasm (Hornung et al., 2008). Cathepsins, in turn, have been observed to promote both priming and activation of the NLRP3 inflammasome (Orlowski et al., 2015). Recently, one of these proteases, cathepsin B, has even been demonstrated to interact directly with NLRP3 to enable inflammasome activation (Chevriaux et al., 2020). While these findings are interesting and may indicate a stimulus-specific NLRP3 activation pathway, it is

certainly difficult to separate the effects of lysosomal rupture from those of ionic flux, since K^+ efflux and Ca^{2+} influx are reportedly induced by lysosomal damage (Katsnelson et al., 2016).

1.3.3.3. Mitochondrial Dysfunction

Mitochondria are the metabolic powerhouse of the cell and must therefore be finely attuned to the cell's changing energetic needs. As a result of their sensitivity and responsiveness to dynamic cellular conditions, mitochondria play a central role in multiple innate immune signaling pathways, including programmed cell death and RIG-I-like receptor-mediated interferon induction (McWhirter et al. 2005; Weinberg et al., 2015). From the earliest days of inflammasome research, it was observed that mitochondria also played an important role in regulation of NLRP3 activation. Virtually all NLRP3 stimuli induce mitochondrial damage, causing mitochondria to release DAMPs, such as reactive oxygen species (ROS) and mitochondrial (mt)DNA (Zhou et al., 2011; Shimada et al., 2012, Liu et al., 2018). Mitochondrial ROS, in particular, have been reported to have a significant impact on NLRP3 function. Multiple studies demonstrated that blocking mitophagy (the selective removal of damaged mitochondria in cells) results in increased mtROS production and triggers NLRP3-mediated IL-1β release (Zhou et al, 2011; van der Burgh et al., 2014). Conversely, when mtROS release was blocked by inhibiting mitochondrial voltage-gated anion channel (VDAC), NLRP3 inflammasome activity was suppressed (Zhou et al., 2011). Notably, two NLRP3 stimuli, imiquimod and CL097, activate the inflammasome through a mechanism dependent on mtROS release, but not on K^+ efflux (Groβ et al., 2016), highlighting the importance of ROS generation in NLRP3 regulation. Another DAMP released by mitochondria is mtDNA. A recent study revealed that inflammasome priming through TLR signaling in macrophages leads to increased mtDNA synthesis (Zhong et al., 2018). When a cell is subsequently treated with an NLRP3 stimulus, this new mtDNA synthesis is necessary for

production and release of oxidized mtDNA from damaged mitochondria (Zhong et al., 2018). Oxidized mtDNA, in turn, binds directly to NLRP3 and promotes NLRP3-mediated IL-1β release (Shimada et al., 2012). Another unique mitochondrial regulator of NLRP3 is hexokinase, a glycolytic enzyme normally localized on the outer mitochondrial membrane. When macrophages or dendritic cells phagocytose Gram-positive bacteria, the pathogen's peptidoglycan breaks down into N-acetylglucosamine (NAG), among other degradation products (Wolf et al., 2016). Cytosolic NAG then binds to hexokinase, causing it to move from mitochondria into the cytosol, where it interacts with NLRP3 and induces inflammasome activation (Wolf et al., 2016). Taken together, these studies provide ample evidence supporting a role for mitochondria in regulation of the NLRP3 inflammasome, particularly in response to specific stimuli. However, defining the precise role of mitochondrial dysfunction and its crosstalk with other cell stress pathways in NLRP3 regulation continues to present a challenge.

1.3.3.4. *Trans*-Golgi Fragmentation

Recent findings have uncovered a role for the Golgi apparatus in activating the NLRP3 inflammasome through cell stress-induced signals. Employing mouse bone marrow-derived macrophage (BMDM) and HeLa cell models, Chen and Chen discovered that NLRP3 stimuli induce fragmentation of *trans*-Golgi membranes, generating structures called the dispersed *trans*-Golgi network (dTGN) (Chen and Chen, 2018). NLRP3 is recruited to these Golgi membranes, where it interacts with a dTGN-associated phospholipid called phosphatidylinositol-4-phosphate (PtdIns4P). This interaction was found to be essential for NLRP3 aggregation and inflammasome signaling (Chen and Chen, 2018). While more investigations into this pathway are needed, it represents a significant advance in our understanding of NLRP3 activation and complements other reported NLRP3 subcellular interactions, which are discussed below.

1.3.4. NLRP3 Subcellular Trafficking

In addition to cellular stress triggers discussed in the preceding sections, ample evidence exists for regulation of NLRP3 through carefully controlled subcellular trafficking events. Several studies revealed that, in response to a priming signal, mitochondria migrate along acetylated microtubules and congregate in a perinuclear region where they come into close association with ER and Golgi membranes (Misawa et al., 2013; Zhang et al., 2017). Physical contact sites between mitochondrial and ER/Golgi membranes are termed ER/Golgi-mitochondria-associated membranes (MAMs). MAMs serve as functional subcellular sites for calcium signaling, lipid synthesis, and innate immune signaling pathways (Horner et al., 2011; Szymanski et al., 2017). Priming and activation signals also cause NLRP3 to relocate from the cytoplasm and ER, where it is localized under resting conditions, to MAM and mitochondrial membranes (Zhou et al., 2011; Zhang et al., 2017, Elliot et al., 2018). Recruitment of NLRP3 to mitochondria and MAMs is mediated by multiple interacting partners. These include MAVS (mitochondrial antiviral signaling protein) and Mitofusin-2, which interact with NLRP3 and regulate its inflammasome activity in response to RNA virus infection (Subramanian et al., 2013; Park et al., 2013; Ichinohe et al., 2013). Another NLPR3 interacting partner is cardiolipin, an inner mitochondrial membrane phospholipid that relocates to the outer mitochondrial membrane in response to inflammasome priming signals and binds directly to NLRP3; this interaction was shown to be necessary for inflammasome activation in response to multiple stimuli (Iyer et al., 2013; Elliot et al., 2018). Microtubule-affinity regulating kinase 4 (MARK4), a regulator of microtubule dynamics, also interacts with NLRP3, promoting its localization to mitochondria and to the microtubule-organizing center (MTOC) (Li et al., 2017), which is closely associated with the Golgi apparatus during interphase (Sanders and Kaverina, 2015). Collectively, all these interacting partners likely serve as molecular scaffolds,

recruiting NLRP3 to the subcellular location where it will be activated. Importantly, procaspase-1 also binds cardiolipin in a mtROS-dependent manner, while ASC interacts with NLRP3 at mitochondria in response to an activating signal through a mechanism that is dependent on Ca^{2+} (Elliot et al., 2018). In this way, priming and activating signals promote trafficking of essential NLRP3 inflammasome components to a common subcellular location, thereby facilitating subsequent inflammasome complex formation. NLRP3 stimulation also induces enrichment of DAG (a downstream product of PLC activity) at Golgi membranes, where it recruits protein kinase D (PKD) (Zhang et al., 2017). Golgi-associated PKD then phosphorylates NLRP3, triggering its release from MAM and mitochondrial membranes (Zhang et al., 2017). Finally, NLRP3 stimulation (signal two) induces dispersal of the *trans*-Golgi network (dTGN), where NLRP3 binds dTGN-associated phosphatidylinositol-4-phosphate (PtdIns4P) (Chen and Chen, 2018). This NLRP3 association with the dTGN may serve as the final destination for NLRP3 trafficking, immediately preceding inflammasome complex formation. Taken together, the aforementioned findings illustrate an intricately orchestrated NLRP3 trafficking pathway induced by priming and activating stimuli, which is governed by cellular stress signals and ultimately culminates in NLRP3-mediated nucleation of a single inflammasome speck.

1.3.5. NLRP3 Post-translational Modifications

Apart from changes in transcription, ionic concentration, organelle function, and subcellular location, NLRP3 activity is also regulated by multiple post-translational modifications, which can promote or inhibit its activation. The E3 ubiquitin ligase TRIM31 (tripartite motif-containing protein 31) interacts with and promotes Lys-48-linked ubiquitination of NLRP3, which targets it for proteasomal degradation and thereby tempers NLRP3 inflammasome activity (Song et al., 2016). Conversely, The Lys-63-specific deubiquitinase BRCC3 (BRCA1/BRCA2-

containing complex subunit 3) deubiquitinates the NLRP3 LRR domain to enable NLRP3 activation (Py et al., 2013). Vitamin D receptor prevents this interaction between NLRP3 and BRCC3, suppressing NLRP3 inflammasome signaling (Rao et al., 2019). NLRP3 is also regulated by phosphorylation. As described in the preceding section, Golgi-localized PKD phosphorylates NLRP3 at Ser295, triggering its release from mitochondrial/MAM membranes and allowing for its subsequent nucleation of the inflammasome complex (Zhang et al., 2017). Meanwhile, PTPN22 (protein tyrosine phosphatase non-receptor 22) dephosphorylates NLRP3 at Tyr861 to promote NLRP3 activation (Spalinger et al., 2016). In addition to ubiquitination and phosphorylation, SUMOylation also plays a role in regulation of NLRP3. The SUMO E3-ligase MAPL (mitochondria-associated protein ligase) sumoylates NLRP3 to inhibit its activation, while the proteins SENP6 (sentrin-specific protease 6) and SENP7 desumoylate NLRP3 to promote inflammasome activity (Barry et al., 2018). Altogether, these modifications highlight the complexity of NLRP3 inflammasome signaling and signify the high molecular licensing threshold that must be met before a cell commits to activating such a consequential inflammatory pathway.

1.3.6. Pyroptosis

An important consequence of NLRP3 inflammasome activation is induction of a lytic pro-inflammatory form of cell death called pyroptosis. Pyroptotic cell death is caspase-dependent and characterized by cell membrane permeabilization, swelling, and rupture. A key molecular determinant of pyroptosis is Gasdermin-D (GSDMD), a bipartite protein consisting of N and C-terminal domains joined by a linker (Shi et al., 2015; He et al., 2016; Liu et al., 2016). Under normal cellular conditions, the C and N-terminal domains associate with each other to maintain GSDMD in an autoinhibited conformation (Ding et al., 2016). In humans, activated caspase-1 or caspase-4/5 cleave the GSDMD linker sequence to release its N-terminal domain, which then self-

oligomerizes to form 10-14 nm pores in the plasma membrane (Liu et al., 2016; Ding et al., 2016). Formation of GSDMD pores facilitates cell swelling and rupture, killing the cell from within (Kovacs and Miao 2017). Cell swelling and rupture are thought to be driven primarily by GSDMD-mediated cell permeabilization, though a recent study has revealed that calpain-dependent loss of cytoskeletal integrity also plays a role in this process, reducing the mechanical resilience of a cell and subjecting it to rupture by physiological shearing forces (Davis et al., 2019). Ultimately, formation of GSDMD pores and subsequent cellular rupture result in release of alarmins, DAMPs, and pro-inflammatory cytokines, such as IL-1β and IL-18, which propagate inflammatory signals to surrounding cells and tissue (He et al., 2016; Monteleone et al., 2018; Davis et al., 2019). Pyroptosis can also defend the host against intracellular pathogens by restricting their ability to replicate within the cell and expelling them into the extracellular space, where they are eliminated by phagocytes (Jorgensen and Miao, 2015). In these ways, NLRP3 inflammasome-mediated cell death can be either protective or harmful, depending on the physiological context and extent to which it is induced. Once again, this highlights the importance of keeping the NLRP3 inflammasome signaling pathway under strict regulatory control.

1.4. Mitochondrial Carrier Proteins

1.4.1. Overview of Mitochondrial Carrier Family

The mitochondrial carrier (MC) family consists of proteins that mediate transport of solutes across the inner mitochondrial membrane (IMM). MC proteins are encoded by nuclear SLC25 genes. Following translation, MCs are trafficked to the IMM by mitochondrial transport machinery; the specificity of their mitochondrial localization is likely determined by an internal targeting sequence within MCs (Ferramosca and Zara, 2013). Once embedded in mitochondria, MCs transport specific solutes across the IMM to supply necessary ions and metabolites for

various metabolic pathways. All MC proteins share a common tripartite structure consisting of three solute carrier (SLC) motifs, each containing two transmembrane helices separated by a linker loop (Ruprecht and Kunji, 2019). Thus, each MC harbors six transmembrane helices, which wrap around to form a barrel-like structure within the IMM, with N and C-termini protruding into the mitochondrial intermembrane space (Ruprecht and Kunji, 2019). To date, fifty-three unique MCs have been identified in humans (Palmieri and Monne, 2016). These can be further separated into 25 subfamilies based on shared sequence homology and transport functions (Palmieri and Monne 2016). One such grouping is the ADP/ATP translocase subfamily, which includes four MC proteins named ANT1/2/3/4 (encoded by SLC25A4/5/6/31 genes). While ANT proteins exhibit different tissue expression patterns, they carry out the same function, namely the exchange of cytoplasmic ADP for mitochondrial ATP (Clemencon et al., 2013). Meanwhile, another carrier, CTP (citrate transporter protein, encoded by the SLC25A1 gene), is the only known human mitochondrial transporter of citrate, a key carbon source for many metabolic pathways (Kaplan et al., 1993; Mosaoa et al. 2021). As investigations into MC proteins progress, they are garnering increased interest in the fields of cancer and metabolism, though little is known about their potential role in immune defense mechanisms.

1.4.2. Mitochondrial Carriers and NLRP3

At least two MC proteins have been implicated in NLRP3 inflammasome regulation. The first is UCP2 (uncoupling protein 2, encoded by the SLC25A8 gene). Sequence similarities led many to assume that UCP2 was a proton channel like UCP1, yet more thorough investigations of UCP2 transport function in liposomes uncovered that it exchanges malate, oxaloacetate, and aspartate for phosphate and a proton across the IMM (Vozza et al., 2014). In one study, mice deficient in UCP2 exhibited improved survival relative to control animals following LPS-induced

sepsis (Moon et al., 2015). The same group then uncovered that UCP2 promoted NLRP3 inflammasome activity in macrophages through upregulation of fatty acid synthase (FASN), which resulted in increased lipogenesis (Moon et al., 2015). Another study observed that UCP2 upregulated NLRP3 expression in THP-1 macrophages, enhancing NLRP3-mediated caspase-1 activation and IL-1β release (Rajanbabu et al., 2015). Thus, UCP2 appears to regulate the NLRP3 inflammasome indirectly through mechanisms involving metabolic pathways and gene transcription. Another reported MC regulator of NLRP3 is ANT1 (encoded by the SLC25A4 gene). When macrophages were stimulated with NLRP3 stimuli, SHP2 (Src homology-2 domain containing protein tyrosine phosphatase-2) was observed to migrate to mitochondria and dephosphorylate ANT1, resulting in mitigation of mitochondrial dysfunction and a tempered inflammasome response (Guo et al., 2017). Deletion of SHP2 from macrophages led to hyperactivation of the NLRP3 inflammasome, while deletion of ANT1 suppressed inflammasome activity (Guo et al, 2017). Thus, ANT1 appears to promote NLRP3 inflammasome activation by facilitating mitochondrial dysfunction. Apart from these reported functions of UCP2 and ANT1, the roles of other MCs in NLRP3 inflammasome regulation have yet to be thoroughly investigated.

1.4.3. Citrin: A Calcium-Sensing Mitochondrial Carrier

In research that will be presented in subsequent sections, we studied the role of an MC called Citrin in regulation of the NLRP3 inflammasome. Citrin (also named AGC2, encoded by the SLC25A13 gene), together with Aralar (also named AGC1, encoded by the SLC25A12 gene), belong to the aspartate/glutamate carrier subfamily of MCs. Functionally, Citrin/Aralar exchange mitochondrial aspartate for cytoplasmic glutamate plus a proton in the IMM (Palmieri et al., 2001). This provides a critical supply of cytosolic aspartate for the urea cycle and purine/pyrimidine synthesis in hepatocytes (Palmieri and Monne 2016). Together with the 2-oxoglutarate carrier

OGC (encoded by the SLC25A11 gene), Citrin/Aralar also play a critical role in the malate-aspartate shuttle (MAS), which mediates the transport of NADH reducing equivalents from the cytosol to the mitochondrial matrix (Amoedo et al., 2016). Structurally, Citrin/Aralar are different from other MCs. In addition to their tripartite carrier domain, Citrin/Aralar also harbor a C-terminal domain with an amphipathic helix and an extended N-terminal domain containing eight EF-hand motifs, only one of which, EF-hand 2, binds a single calcium ion (Thangaratnarajah et al., 2014). Structural modeling of Citrin and Aralar revealed that, upon calcium binding, the C-terminal domain binds to the N-terminal region to open a vestibule, allowing solutes to enter the carrier. When calcium was not bound, this vestibule was closed (Thangaratnarajah et al., 2014). This complemented previous studies in which calcium binding to the N-terminal domain was shown to be necessary for optimal aspartate/glutamate transport activity (Contreras et al., 2007; Marmol et al., 2009). Surprisingly, the Citrin/Aralar N-terminal domain was also found to facilitate self-dimerization, a novel observation for MC proteins (Thangaratnarajah et al., 2014). While they have similar structures and function, Citrin and Aralar exhibit different tissue distribution patterns. Both are expressed quite ubiquitously, though Aralar is found predominantly in brain, heart, and skeletal muscle, while Citrin is highly expressed in the liver and kidney (del Arco and Satrustegui 1998; del Arco et al., 2000). This tissue distribution pattern tracks closely with diseases in which these proteins are implicated. Aralar deficiency has been associated with hypomyelination in the central nervous system, developmental delay, and autism (Wibom et al., 2009; Palmieri 2014). Citrin deficiency, meanwhile, causes congenital liver diseases, namely neonatal intrahepatic cholestasis by citrin deficiency (NICCD) and adult-onset type-II citrullinemia (CTLN2), both of which arise due to a shortage of cytosolic aspartate and a dysfunctional MAS (Saheki and

Kobayashi 2002; Palmieri 2014). To date, however, a functional role for Citrin or Aralar in NLRP3 inflammasome regulation has not been described.

1.5. Unanswered Questions

Multiple studies have established that NLRP3 is recruited to mitochondria and MAM membranes upon inflammasome priming or stimulation (Zhou et al., 2011; Subramanian et al., 2013; Ichinohe et al., 2013; Elliot et al., 2018). However, actual NLRP3 aggregation and inflammasome complex formation appears to occur on disrupted *trans*-Golgi membranes (Chen and Chen 2018). To reconcile these observations, some have proposed that MAM and mitochondria serve as docking sites for NLRP3, effectively trafficking NLRP3 into closer proximity to the Golgi, where it will be nucleated. To date, only a few mitochondrial components, namely cardiolipin, MAVS, and Mitofusin-2, have been demonstrated to interact with NLRP3 to promote its mitochondrial localization (Iyer et al., 2013; Subramanian et al., 2013; Ichinohe et al., 2013). While cardiolipin is necessary for NLRP3 inflammasome activation in the context of multiple NLRP3 stimuli (Iyer et. al., 2013; Elliot et al., 2018), MAVS and Mitofusin-2 appear important for NLRP3 inflammasome activity only in response to RNA virus infection or treatment with the RLR agonist poly(I:C), but not in response to other stimuli, such as MSU, nigericin, or ATP (Park et al., 2013; Ichinohe et al., 2013, Franchi et al., 2014). It would be useful to uncover whether or not other mitochondrial components interact with NLRP3 and assist in its recruitment to mitochondrial and MAM membranes, with consequential outcomes on inflammasome activation in response to a wide range of NLRP3 stimuli.

Two mitochondrial carrier proteins, UCP2 and ANT1, have been implicated in molecular regulation of NLRP3 inflammasome activity (Moon et al., 2015; Guo et al., 2017). The role of the other fifty-one human mitochondrial carriers in NLRP3 regulation has not been thoroughly

researched, though many of them perform transport functions that are critical for cellular metabolic pathways and maintenance of mitochondrial homeostasis, perturbations of which are known to promote NLRP3 inflammasome activation (Zhou et al., 2011; van der Burgh et al., 2014; Shimada et al., 2012; Wolf et al., 2016). Some, like Citrin and Aralar, are sensitive to changes in cytosolic Ca^{2+} concentration, which reportedly impacts NLRP3 activity (Lee et al., 2012; Murakami et al., 2012). For these reasons, after uncovering a link between mitochondrial carriers and NLRP3 through a proteomics screen, we proceeded to investigate their role in NLRP3 inflammasome regulation.

In what follows, we present evidence for molecular regulation of the NLRP3 inflammasome by the mitochondrial carrier Citrin. Our studies reveal a newly discovered interaction between Citrin and NLPR3, which may facilitate NLRP3 recruitment to MAM membranes. We also demonstrate that Citrin deletion suppresses NLRP3-specific inflammasome IL-1β release, pyroptotic cell death, and ASC speck formation, while Citrin overexpression induces NLRP3 inflammasome activation. Altogether, our findings identify Citrin to be a new mitochondrial regulator of the NLRP3 inflammasome signaling pathway.

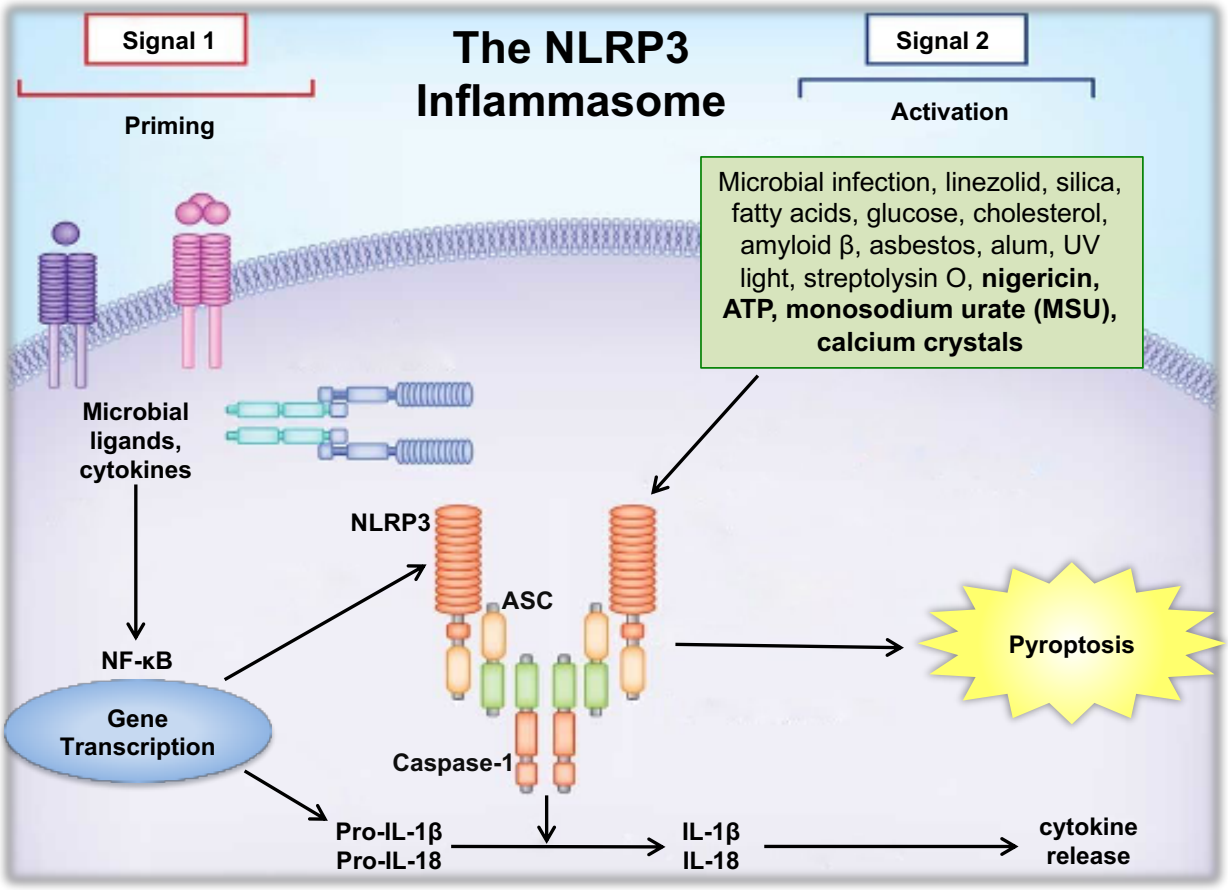

Figure 1.1. The NLRP3 Inflammasome Signaling Pathway. Overview of key signaling events in the NLRP3 inflammasome pathway. The priming signal is initiated when microbial ligands or cytokines engage PRR receptors, inducing NFkB-mediated upregulation of NLRP3, proIL-1β, and other inflammatory mediators. Signal two can then be supplied by many different stimuli, some of which are listed in this figure, resulting in NLRP3 activation and inflammasome complex assembly with ASC and procaspase-1. Formation of the inflammasome activates caspase-1, leading to cleavage and release of pro-inflammatory cytokines IL-1β and IL-18 and induction of pyroptotic cell death.

2. The mitochondrial carrier Citrin interacts with NLRP3 and regulates its inflammasome activity

Andrey Shuvarikov, Michael Davis, Katharina Esser-Nobis, Sean White and Michael Gale, Jr.

2.1. Introduction

The Nod-like receptor family, pyrin domain-containing 3 (NLRP3) protein is a cytosolic pattern recognition receptor (PRR) that initiates formation of an inflammasome complex in response to pathogenic, environmental, or host-derived threats (Schroder and Tschopp, 2010; Swanson et al., 2019). Once activated, NLRP3 self-oligomerizes and associates with apoptosis-associated speck-like protein (ASC), which recruits the cysteine protease caspase-1 to form an inflammasome complex. Assembly of this complex activates caspase-1, which cleaves pro-interleukin-1β (proIL-1β) and proIL-18 into their active secreted forms (Latz et al., 2013; Sutterwala et al., 2014). Once released from the cell, the pro-inflammatory IL-1β and IL-18 cytokines promote a wide range of immune responses, including cell-intrinsic defense pathways, neutrophil recruitment, and activation of T cells (Dinarello 2009). Inflammasome activation also induces pyroptosis, a pro-inflammatory form of cell death characterized by membrane permeabilization, cell swelling and rupture (Yu et al., 2021). While multiple inflammasome sensors have been identified in humans, NLRP3 has garnered particular interest due to its importance in human health and disease. As a molecular regulator of inflammation, NLRP3 plays a critical role in pathogen clearance and tissue repair, yet has also been linked to multiple inflammatory disorders, including cryopyrin-associated periodic syndromes (CAPS), Type 2 diabetes, atherosclerosis, Alzheimer's, and gouty arthritis (Lamkanfi and Dixit, 2012; Strowig et al., 2012).

In nearly all cases, the NLRP3 inflammasome requires two signals for its activation. The first signal primes the cell for the inflammasome response. This priming signal can be supplied by microbial ligands binding to toll-like receptors (TLRs) or NOD2, as well as by cytokines such as tumor necrosis factor-α (TNF-α) or IL-1β (Bauernfeind et al., 2009; Franchi et al., 2009). Signaling pathways triggered by these stimuli activate the transcription factor NF-κB, which induces increased expression of both proIL-1β and NLRP3 (Bauernfeind et al., 2009; He et al., 2016). In addition to transcriptional changes, priming also induces post-translational modifications to NLRP3 necessary for its activation (Seok et al., 2021). Together, these changes prepare the cell for the second signal, which activates NLRP3 and triggers assembly of the inflammasome complex. This second signal can be supplied by a multitude of chemically different stimuli. These include, among others, pathogen-associated molecular patterns (PAMPs), pore-forming toxins, environmental or host-derived particulates, and damage-associated molecular patterns (DAMPs), such as extracellular ATP (Mariathasan et al., 2006; Martinon et al., 2006; Dostert et al., 2008; Hornung et al., 2008; Halle et al., 2008; Harder et al., 2009; Schroder and Tschopp, 2010). The precise mechanism by which these different stimuli activate NLRP3, however, remains elusive and continues to present a central enigma in the inflammasome field. While being chemically unrelated, all known NLRP3 stimuli converge in their ability to elicit cellular stress. It is postulated that specific cellular perturbations associated with this cellular stress likely serve as the activating signal(s) of NLRP3. These cellular disruptions include intracellular ionic flux, lysosomal rupture, Golgi disassembly, and mitochondrial dysfunction (Muñoz-Planillo et al., 2013; Murakami et al., 2012; Hornung et al., 2008; Chen and Chen, 2018; Zhou et al., 2011). As investigations progress into how these cellular perturbations regulate NLRP3 activation, many studies continue to focus

on mitochondria, as more discoveries implicate them to be central players in the NLRP3 inflammasome signaling pathway (Gurung et al., 2015, Liu et al., 2018).

Mitochondria impart their regulation on the NLRP3 inflammasome through multiple fronts. Nearly all NLRP3 stimuli induce some level of mitochondrial dysfunction. When mitophagy is inhibited, preventing cells from effectively clearing damaged mitochondria, this leads to NLRP3 inflammasome activation, underscoring the importance of mitochondrial dysfunction in inflammasome regulation (Zhou et al., 2011; van der Burgh et al., 2014). Dysfunctional mitochondria also release mitochondrial reactive oxygen species (mtROS) and oxidized mitochondrial DNA (ox-mtDNA) into the cytosol, DAMPs which promote NLRP3 activation (Zhou et al., 2011; Shimada et al., 2012). Further evidence shows that NLRP3 is recruited to mitochondrial membranes in response to specific priming or activating signals, where it interacts with various mitochondrial components, including mitochondrial antiviral signaling protein (MAVS), Mitofusin-2, and the phospholipid cardiolipin (Subramanian et al., 2013; Ichinohe et al., 2013; Iyer et al., 2013). While NLRP3 recruitment to mitochondria and responsiveness to mitochondrial DAMPs are necessary for optimal inflammasome activity in certain contexts, the precise role of mitochondria in regulating NLRP3 activation still needs to be fully defined.

Citrin (also known as SLC25A13 or AGC2) is a six-pass transmembrane protein localized in the inner mitochondrial membrane. Citrin belongs to a large family of mitochondrial solute carrier (SLC25) proteins, with which it shares homology in structure and sequence (Palmieri 2013, Amoedo et al., 2016). Functionally, Citrin mediates the calcium-dependent exchange of mitochondrial aspartate for cytoplasmic glutamate. This transport activity plays an important role in the urea cycle and is an integral step in the malate-aspartate shuttle (MAS), which serves to

replenish supplies of NADH reducing equivalents in the mitochondrial matrix (Palmieri et al., 2001). In humans, Citrin deficiency can cause neonatal intrahepatic cholestasis caused by Citrin deficiency (NICCD) and adult-onset type II citrullinemia (CTLN2); both are serious diseases caused by metabolic deficiencies in the liver (Saheki and Kobayashi, 2002). While specific mitochondrial carrier proteins, such as ANT1 (SLC25A4) and UCP2 (SLC25A8) have been identified as NLRP3 inflammasome regulators (Guo et al., 2017; Rajanbabu et al., 2015), a functional association between Citrin and the NLRP3 inflammasome has not yet been described. In this study, we identify Citrin as an interactor of NLRP3 and a regulator of its inflammasome activity. Our findings uncover a new mechanism for mitochondrial regulation of the NLRP3 inflammasome and reveal a newly discovered function for Citrin.

2.2. Results

2.2.1. A proteomic link between NLRP3 and Citrin

To gain new insights into cellular mechanisms regulating the NLRP3 inflammasome pathway, we performed a proteomics screen to identify protein interactors of NLRP3 (**Figure 2.1A**). N or C-terminally FLAG-tagged NLRP3 was exogenously expressed in HEK-293A cells either alone or together with the inflammasome components ASC and pro-Caspase-1. Transfection of all expression plasmids was performed using calcium phosphate, a known activator of the NLRP3 inflammasome (Pazar et al., 2011). To minimize proteolytic damage, we expressed procaspase-1 harboring a C285A mutation, which inhibits its proteolytic function while maintaining its ability to interact with the inflammasome complex (Lamkanfi et al., 2004). Lysates from these cells were subjected to anti-FLAG immunoprecipitation, followed by mass spectrometric analysis to identify NLRP3-interacting proteins. Using this screen, we identified multiple high confidence NLRP3 interactors, including the previously reported NLRP3

inflammasome regulators, NEK7 and SUGT1 (He et al., 2016; Mayor et al., 2007), as well as the co-expressed inflammasome proteins ASC and procaspase-1 (**Figure 2.1B**). Surprisingly, we also identified four mitochondrial solute carrier proteins to be high confidence interactors of NLRP3. These included CTP (a citrate transporter), ANT3 (an ADP/ATP translocase), OGC (a 2-oxoglutarate/malate carrier), and Citrin (a calcium-dependent aspartate/glutamate transporter) (**Figure 2.1B**).

Subsequent co-immunoprecipitation (co-IP) experiments using FLAG-tagged NLRP3 co-expressed with V5-tagged CTP, ANT3, OGC, or Citrin in HEK-293A confirmed that these four mitochondrial carriers interacted with NLRP3 (**Figure 2.1D**). To explore a possible association between the identified interactors and NLRP3-linked diseases, genes for CTP, ANT3, OGC, and Citrin were queried in the GWAS Central database, which reports links between specific genes and genome-wide association studies (Beck et al., 2020). Intriguingly, only one of the mitochondrial carriers, Citrin, exhibited substantial overlap with the same genetic association studies and diseases with which NLRP3 and NEK7 were also linked (**Table S1**). Citrin was also notably different from CTP, ANT3, and OGC in its domain structure, sharing a similar carrier domain, but harboring extended N-terminal and C-terminal domains that distinguished it from the other carriers (**Figure 2.1C**). Furthermore, Citrin's N-terminal domain harbors a calcium-binding EF-hand motif, which enables it to respond to changes in cytosolic calcium concentrations (Palmieri et al., 2001, Amoedo et al., 2016). Taking into account these unique features of Citrin, as well as its proteomic and GWAS associations with NLRP3, we set out to investigate whether Citrin was playing a role in regulation of the NLRP3 inflammasome.

2.2.2. Citrin interacts with NLRP3 via its solute carrier domain

To begin, we performed a series of co-IP experiments to further characterize the interaction between NLRP3 and Citrin. Following co-expression of V5-tagged Citrin and FLAG-tagged NLRP3 in HEK-293A cells, Citrin-V5 co-immunoprecipitated with N and C-terminally FLAG-tagged NLRP3; conversely, NLRP3-FLAG co-immunoprecipitated with Citrin-V5 (**Figures 2.2A, 2.2B**). This data validated the interaction initially identified in our proteomics screen. We then tested whether or not Citrin interacted with inflammasome components other than NLRP3. Interestingly, Citrin-V5 co-immunoprecipitated with FLAG-tagged proIL-1β, but not with FLAG-tagged ASC or procaspase-1 (**Figure 2.2B**). This suggests a mechanism in which Citrin interacts with both the sensor and effective substrate of the NLRP3 inflammasome.

Next, we defined the domains of NLRP3 and Citrin necessary for their interaction. To do this, we generated truncated mutants of Citrin and NLRP3, as well as functional mutants of Citrin (**Figures 2.2C, 2.2E**). Human Citrin is a 74 kDa protein comprised of three major domains. It has a central solute carrier domain, which contains six transmembrane helices and serves as the site of solute transport. Citrin also harbors a C-terminal domain containing an α-helix and a calcium-responsive N-terminal domain housing eight EF-hand motifs, one of which binds a calcium ion (Thangaratnarajah et al., 2014). Plasmids were generated expressing V5-tagged Citrin constructs. These included full-length Citrin, Citrin with truncated N-terminal, C-terminal, or N and C-terminal domains, full-length Citrin harboring E28A/N30A/D66A/T68A mutations that prevented it from binding calcium (Marmol et al., 2009; Thangaratnarajah et al., 2014), and Citrin with a Q592R mutation that disabled it from transporting solutes (Wibom et al., 2009) (**Figure 2.2C**). Surprisingly, all Citrin constructs co-immunoprecipitated with NLRP3-FLAG in HEK-293T cells, demonstrating that the Citrin carrier domain was sufficient for binding with NLRP3, while calcium responsiveness and transport function were not necessary for this interaction (**Figure 2.2D**). A

similar analysis was performed with NLRP3, which was truncated into its N-terminal pyrin (PYD), central NACHT, and C-terminal leucine-rich repeat (LRR) domains, as well as the linker sequences by which these domains are separated (**Figure 2.2E**). Citrin-V5 co-immunoprecipitated most strongly with the NLRP3 LRR domain and its adjacent linker sequence **(Figure 2.2F)**, a region of NLRP3 that is also necessary for its interaction with NEK7 (He et al., 2016). Taken together, these studies reveal that the NLRP3-Citrin interaction is mediated through their LRR and carrier domains, respectively **(Figure 2.2G)**.

2.2.3. NLRP3 stimulation increases Citrin localization at the MAM

The endoplasmic reticulum (ER)-mitochondria-associated membrane (MAM) is a distinct subcellular compartment in which mitochondrial membranes come into close, physical contact with the ER. Functionally, the MAM plays an important role in lipid synthesis, calcium signaling, and innate immune signaling pathways (Horner et al., 2011; Szymanski et al., 2017). Multiple studies have reported that NLRP3 localizes to MAM and mitochondrial membranes in response to NLRP3 inflammasome priming and stimulation (Zhou et al., 2011; Subramanian et al., 2013; Elliot et al., 2018). Because Citrin localizes at the inner mitochondrial membrane, while NLRP3 is predominantly cytoplasmic under normal cellular conditions, we asked whether or not Citrin was localizing to a different subcellular location in response to NLRP3 inflammasome stimulation. To answer this, we performed subcellular fractionation of THP-1 cells, a human monocytic cell line commonly used in inflammasome studies. THP-1 cells were differentiated into macrophages using phorbol myristate acetate (PMA), then treated with nigericin, a pore-forming toxin that activates the NLRP3 inflammasome. Treated cells were fractionated into cytoplasmic, mitochondrial, microsomal, and MAM fractions using a previously described protocol (Bozidis et al., 2007) (**Figure 2.3A**). Following nigericin treatment, we observed approximately a two-fold increase in

Citrin protein levels in the MAM fraction, together with a substantial loss of proteins in the mitochondrial fraction (**Figures 2.3B, 2.3C**). Thus, nigericin-induced NLRP3 stimulation increased Citrin localization at the MAM, revealing to be a potential subcellular compartment where the Citrin-NLRP3 interaction takes place.

2.2.4. Citrin is required for optimal NLRP3 inflammasome activity in THP-1 macrophages

After characterizing Citrin's interaction with NLRP3, we tested whether or not Citrin had a functional effect on NLRP3 inflammasome activity. Using CRISPR/Cas9 technology, we generated NLRP3, Citrin, and ANT3 knockout (ko) THP-1 cell lines (**Figure 2.4A**). THP-1 cells transduced with non-targeting CRISPR gRNA (NTC cells) were used as the reference cell line (**Figure 2.4A**). ANT3 ko cells were generated to test the effect of deleting another mitochondrial carrier identified as an NLRP3 interactor in our proteomics screen (**Figures 2.1B, 2.1C**), but one which lacked association with NLRP3-linked GWAS studies and diseases (**Table S1**). PMA-differentiated THP-1 macrophages were primed with LPS and treated with four chemically different activators of the NLRP3 inflammasome: nigericin, ATP, monosodium urate (MSU) crystals, and UV-inactivated hepatitis C virus (UV HCV). Following treatments, IL-1β release was measured in cell supernatants by ELISA and immunoblot. Citrin ko THP-1 macrophages exhibited a significant reduction in released IL-1β relative to control cells following treatment with either of the four NLRP3 stimuli (**Figure 2.4B, 2.4D**). As expected, IL-1β release from NLRP3 ko cells was nearly completely abrogated, while IL-1β release from ANT3 ko cells was surprisingly not significantly affected relative to control cells (**Figure 2.4B, 2.4D**). Citrin deletion, meanwhile, did not impact intracellular expression levels of NLRP3, procaspase-1, or proIL-1β following LPS priming, which remained similar to those of NTC cells (**Figure 2.4E**). Citrin deletion also did not

affect IL-1β release in response to the AIM2 inflammasome activator poly(dA:dT) (**Figure 2.4C**), indicating that Citrin's regulatory activity was specific to NLRP3 stimuli.

In addition to cytokine release, the NLRP3 inflammasome also induces pyroptosis, a proinflammatory form of cell death initiated by caspase-1-mediated cleavage of Gasdermin-D, which forms pores in the plasma membrane, leading to cell swelling and release of inflammatory cytokines (Shi et al., 2015; He et al., 2016; Liu et al., 2016). To test the effect of Citrin deletion on NLRP3-mediated cell death, we quantified dead cells by measuring uptake of a cell-impermeable SYTOX-Green fluorescent dye using a live-cell imager (**Figure 2.5A**). Following treatment with the NLRP3 stimuli, nigericin, MSU, and UV HCV, Citrin ko THP-1 macrophages exhibited a marked reduction in cell death relative to control cells (**Figure 2.5C**), while nigericin-treated ANT3 ko cells did not (**Figure 2.5B**). Citrin ko macrophages, however, showed no change in cell death levels from control cells following treatment with the AIM2 stimulus poly(dA:dT) or activators of apoptotic and necroptotic cell death pathways (**Figure 2.5D, 2.5E**). Thus, Citrin-mediated regulation of cell death appeared specific to pyroptosis induced by NLRP3 stimuli.

Seeing that Citrin deletion suppressed IL-1β release and cell death, which are events downstream of NLRP3 inflammasome activation, we investigated whether or not Citrin affected formation of the NLRP3 inflammasome complex itself. To study this, we generated NTC, NLRP3 ko, and Citrin ko THP-1 cells stably expressing mCherry-tagged ASC (**Figure 2.6A**). This enabled us to quantify inflammasome complexes, which could be visualized as single ASC specks within cells, using a live-cell imager (**Figure 2.6B**). THP-1 CRISPR cells expressing mCherry-ASC were stimulated with the NLRP3 stimuli nigericin and UV HCV. As was observed with IL-1β release and cell death, Citrin ko cells demonstrated a significant reduction in ASC speck formation relative

to control cells (**Figure 2.6C**). This provided evidence that Citrin imparted its regulatory activity on NLRP3 upstream of inflammasome complex formation.

2.2.5. Overexpressed Citrin promotes NLRP3 inflammasome activation via its N-terminal domain

After observing that Citrin deletion significantly suppressed NLRP3 inflammasome activity, we hypothesized that Citrin overexpression could induce it. To test this, we ectopically expressed FLAG-tagged NLRP3, procaspase-1, ASC, and proIL-1β in HEK-239A cells to reconstitute these cells with essential components of the NLRP3 inflammasome. Overexpression of V5-tagged Citrin triggered release of cleaved IL-1β from these cells, while overexpression of FLAG-tagged GFP and V5-tagged ANT3 did not (**Figures 2.7A, 2.8A**). Citrin-induced release of IL-1β was dependent on the NLRP3 inflammasome, as it required the presence of NLRP3, procaspase-1, and ASC (**Figure 2.7A**). Citrin-V5 overexpression also induced formation of inflammasome specks in HEK-293A cells, but only when it was co-expressed with NLRP3 and ASC (**Figure 2.8B**). A more magnified examination of these specks revealed close apposition between the NLRP3-ASC speck and mitochondrial membranes where Citrin-V5 was localized (**Figure 2.8C**). Mitochondrial membranes, which stained strongly for Citrin-V5, appeared to wrap around the inflammasome complex and make contact with its periphery (**Figure 2.8D**).

We then asked whether calcium-binding, solute transport activity, or a specific domain of Citrin was important for its promotion of NLRP3 inflammasome activity in HEK-293A cells. V5-tagged Citrin mutants described previously (see **Figure 2.2C**) were overexpressed in HEK-293A cells with reconstituted NLRP3 inflammasomes, followed by quantification of IL-1β release and inflammasome speck frequency (**Figures 2.7C, 2.7D and 2.7E**). All overexpressed Citrin mutants

co-localized well with mitochondria, as could be seen when co-staining V5-tagged Citrin constructs with the mitochondrial marker TOM20 (**Figure 2.9**). Intriguingly, only the truncation of Citrin's N-terminal domain abrogated its ability to induce cleaved IL-1β release and inflammasome speck formation, while truncation of the C-terminal domain and mutations preventing calcium binding and transport activity did not affect this induction of inflammasome activity (**Figures 2.7C, 2.7D and 2.7E**). These observations indicate that overexpressed Citrin promotes NLRP3 inflammasome activation through a mechanism that relies on its N-terminal domain, but for which its transport and calcium-binding activities are not required.

2.3. Discussion

Collectively, our findings reveal Citrin to be a mitochondrial regulator of the NLRP3 inflammasome. Our observations support a model in which NLRP3 inflammasome stimulation triggers increased Citrin localization at MAM membranes, enabling Citrin to interact with NLRP3 and promote nucleation of the NLRP3 inflammasome complex (**Figure 2.8**).

Using proteomics and co-IP approaches, we uncovered a previously unreported interaction between NLRP3 and Citrin (see **Figures 2.1, 2.2**). Employing protein truncations, we found that the solute carrier domain of Citrin was sufficient for its NLRP3 interaction (**Figure 2.2D**). This finding was supported by our proteomics data, since the carrier domain is the only region of homology that Citrin shares with the other identified mitochondrial carrier interactors of NLRP3, namely CTP, ANT3, and OGC (see **Figure 2.1**). We also found that the C-terminal LRR domain of NLRP3 was necessary for its interaction with Citrin (**Figure 2.2E**). In this respect, Citrin was different from MAVS, which reportedly interacted with the N-terminal PYD domain of NLRP3

(Subramanian et al., 2013). Yet, Citrin shared some similarities with NEK7 and cardiolipin, which are also reported to interact with the NLRP3 LRR domain (He et al., 2016; Sharif et al., 2019; and Iyer et al., 2013). Surprisingly, we found that Citrin interacted not just with NLRP3, but also with proIL-1β. Though it is tempting to speculate that Citrin's interaction with pro IL-1β may serve to bring the inactive cytokine into closer proximity to the site of NLRP3 inflammasome nucleation, thereby facilitating its subsequent cleavage by caspase-1, more investigations into Citrin's interaction with IL-1β are needed.

Interaction of Citrin, an inner mitochondrial membrane carrier, with NLRP3, which resides predominantly in the cytoplasm or at ER membranes in resting cells (Zhou et al., 2011), presents a conundrum, as these two proteins should not come into contact with each other under normal cellular conditions. Multiple studies have demonstrated that NLRP3 localizes strongly to MAM and mitochondrial membranes in response to both priming and activating NLRP3 signals (Zhou et al., 2011; Subramanian et al., 2013; Iyer et al., 2013; Elliot et al., 2018). However, even when NLRP3 localizes to mitochondria, it reportedly binds to the outer mitochondrial membrane (OMM) rather than inner mitochondrial membrane (IMM) (Elliot et al., 2018). Our observation that Citrin localization increases at the MAM following nigericin stimulation of THP-1 macrophages (see **Figure 2.4**) presents a possible solution to this puzzle, suggesting a mechanism in which Citrin interacts with NLRP3 at MAM membranes. Relocation of mitochondrial components to a different subcellular compartment is not unprecedented, particularly in the context of NLRP3 inflammasome activation. Cardiolipin is a mitochondrial lipid that translocates from the inner to outer mitochondrial membrane in response to NLRP3 stimuli, where it subsequently interacts with NLRP3 and procaspase-1 (Iyer et al., 2013, Elliot et al., 2018). In a study performed by Wolf et al., N-acetylglucosamine, a degradation product of bacterial peptidoglycan, inhibited

hexokinase, causing it to move from the OMM to the cytosol, where it was sufficient to trigger NLRP3 activation (Wolf et al., 2016). Indeed, Citrin has itself been reported to traffic in and out of MAM membranes, along with other mitochondrial carriers, following RNA virus infection of Huh7 and PH5CH8 cells (Horner et al., 2015). Thus, movement of mitochondrial components to other subcellular compartments occurs and could serve as an intracellular signal of danger or damage that is sensed by NLRP3, culminating in its eventual nucleation of the inflammasome complex. Our own observations that overexpressed Citrin promoted NLRP3 inflammasome activity in HEK-293A cells (see **Figure 2.7**) may have been a result of overexpression-driven localization of Citrin to the OMM or MAM, though more in-depth studies are needed to confirm this. While all overexpressed Citrin mutants appeared to co-localize with mitochondria (**Figure 2.9**), it was not possible to discern IMM vs OMM or MAM localization with the imaging resolution used. Thus, further studies will be needed to unravel the precise mechanisms for Citrin's subcellular relocation and interaction with NLRP3.

Our investigations revealed that Citrin plays a functional role in regulating the NLRP3 inflammasome. Citrin deletion from THP-1 cells resulted in a significant suppression of NLRP3 inflammasome activity, as evidenced by reduced IL-1β release, pyroptotic cell death, and ASC speck formation (see **Figures 2.4, 2.5 and 2.6**). However, Citrin deletion did not induce a complete abrogation of NLRP3 inflammasome function, indicating that Citrin was an important but not indispensable determinant of NLRP3 inflammasome complex formation. While Citrin deletion suppressed NLRP3 inflammasome signaling, overexpression of Citrin in HEK-239A cells with reconstituted inflammasomes induced robust NLRP3 inflammasome activation, signified by release of cleaved IL-1β and formation of inflammasome specks (see **Figure 2.7**). Unexpectedly, this promotion of NLRP3 activity was dependent on Citrin's N-terminal domain, but not its ability

to bind calcium or transport solutes (**Figures 2.7C, 2.7E**). In addition to harboring the calcium-binding site, the N-terminal domain also plays an important role in Citrin homodimerization and transport function (Thangaratnarajah et al., 2014). It is possible that the N-terminal domain is also important for Citrin's localization at the MAM. Further studies will be needed to elucidate the precise mechanism by which Citrin's N-terminal domain enables it to regulate the NLRP3 inflammasome. While we cannot discount a role for mitochondrial dysfunction and metabolic changes in Citrin-mediated regulation of NLRP3 activity, our findings that the transport-incapable Q592R Citrin mutant still interacted with NLRP3 and promoted inflammasome activation suggest that Citrin's solute transport function may not be necessary for its regulation of NLRP3.

To date, multiple studies have implicated mitochondria to be important regulators of the NLRP3 inflammasome (reviewed in Gurung et al., 2015; Liu et al., 2018), postulating even that MAM and mitochondrial membranes serve as subcellular platforms for NLRP3 inflammasome nucleation (Missiroli et al., 2018). However, a 2018 study by Chen and Chen challenged the role of mitochondria in NLRP3 activation, reporting instead that NLRP3 inflammasomes are nucleated on dispersed *trans*-Golgi network (dTGN) membranes, which become dissociated in response to NLRP3 stimuli (Chen and Chen, 2018). We propose a consensus model for NLRP3 activation that reconciles these seemingly contradictory findings and also defines a role for Citrin. When a macrophage is licensed for NLRP3 inflammasome activation via a priming signal, multiple events have been reported to occur. First, NLRP3 is recruited to mitochondrial and MAM membranes through its interaction with cardiolipin, and possibly also through its interaction with MAVS and Mitofusin-2 (Iyer et al., 2013; Subramanian et al., 2013; Park et al., 2013; and Ichinohe et al., 2013). Citrin may similarly be functioning as a scaffolding protein by helping to recruit NLRP3 to these subcellular compartments. Second, the priming signal also induces mitochondria to migrate

along acetylated microtubules toward the perinuclear region (Misawa et al., 2013), where they come into close proximity to Golgi membranes (Zhang et al., 2017). In this subcellular region, phosphokinase D (PKD) phosphorylates NLRP3, releasing it from mitochondrial membranes and allowing it to interact with the Golgi (Zhang et al., 2017). Finally, NLRP3 stimuli that supply the second signal induce dispersal of the *trans*-Golgi network, generating fragmented Golgi vesicles, which may then serve as nucleation sites for the NLRP3 inflammasome (Chen and Chen, 2018). Thus, in our proposed model, mitochondria and MAM membranes, acting through NLRP3 interactors such as cardiolipin and Citrin, serve as docking platforms, recruiting NLRP3 to the subcellular location where the inflammasome will be nucleated.

In conclusion, we have identified Citrin to be a newly discovered interactor of NLRP3 and a regulator of its inflammasome activity. Our findings provide new insights into mitochondrial regulation of the NLRP3 inflammasome and unveil a previously unreported function for Citrin. These findings enhance our understanding of the molecular mechanisms governing NLRP3 inflammasome activation and may be leveraged clinically by identifying a new target for anti-inflammatory therapeutics.

2.4. Materials and Methods

Cell Culture and Viruses

HEK-293T (ATCC; CRL-3216), THP-1 (ATCC; TIB-202), HEK-293A (ThermoFisher; R70507), and Huh7.5 cells (described by Pflugheber et al., 2002) were cultured at 37°C, 5% CO_2 using standard techniques. HEK-293A and HEK-293T cells were grown in Dulbecco's Modified Eagle Medium (DMEM) supplemented with 10% fetal bovine serum (FBS), L-glutamine, nonessential

amino acids, sodium pyruvate, and penicillin/streptomycin. THP-1 cells were cultured in Roswell Park Memorial Institute (RPMI) 1640 Medium supplemented as above, except with 10% heat-inactivated FBS. Human hepatitis C virus (HCV) was grown and titered in Huh7.5 cells as described by Kato et al., 2006. To inactivate HCV, viral stocks or virus-containing supernatants were UV irradiated at 1200mJ/cm2 for 30 minutes using a UV Stratalinker. All cell lines and viral stocks were verified to be mycoplasma-free using the MycoAlert Mycoplasma test kit (Lonza; LT07-318).

Reagents and Cell Treatments

Phorbol 12-Myristate 13-Acetate (PMA) (Sigma; P8139) was dissolved in DMSO to make a 200 μM stock. THP-1-derived macrophages were generated by treating cells with 40 nM PMA for 16 hours, then washing with 1X PBS and "resting" the cells 24 hours in RPMI medium without PMA. All THP-1 treatments described below were performed after the 24-hour rest period. Ultrapure LPS from E. coli 0111:B4 (Invivogen; tlrl-3pelps) was dissolved in endotoxin free water to 1 mg/mL and used at a concentration of 5 ng/ml to prime THP-1 cells. Nigericin (Sigma; N7143) was dissolved in methanol to 10 mM and used at 10 μM, ATP solution (Sigma; A6559) was used at 5 mM, while monosodium urate salt was resuspended in 1X PBS to 20 mg/mL and used at 300 μg/ml to stimulate the NLRP3 inflammasome. Poly(dA:dT) (Invivogen; tlrl-patn) was reconstituted with physiological water to 1 mg/mL and transfected into THP-1 cells at 2 μg/ml using Lipofectamine 2000 reagent (Thermofisher; 11668030), according to the manufacturer's protocol. For inflammasome stimulation experiments, unless otherwise specified, PMA-differentiated THP-1 macrophages were seeded at 5x10^4 cells/well in 96-well plates, primed 4 hours with LPS, then treated with AIM2 or NLRP3 stimuli for specified times. For cell death assays, recombinant human TNF-α (PeproTech; 300-01B) was reconstituted in PBS to 100 μg/ml

and used at 100 ng/ml, zVAD (SM Biochemicals; SMFMK001) was dissolved in DMSO to 50 mM and used at 50 μM, BV6 (ApexBio; B4653), a selective inhibitor of IAP proteins, was used at 1 μM, while cycloheximide (Sigma; B4859) was used at 10 μg/mL to treat THP-1 macrophages.

Mass Spectrometry and Proteomics

Plasmids expressing N or C-terminally FLAG-tagged human NLRP3 were transfected, either alone or with plasmids expressing ASC and procaspase-1 (C285A mutant), into HEK-293A cells by Ca-PO_4 transfection, using standard techniques. Transfections were performed in duplicate. 48 hours post-transfection, cells were harvested in 0.5% NP-40 lysis buffer (0.5% Nonidet P-40, 1 mM EDTA, 1 mM PMSF, 250 μM okadaic acid, 1:100 protease inhibitor mixture (Sigma; P3340), and 1:1000 phosphatase inhibitor cocktail (Calbiochem; 524625). FLAG-tagged NLRP3 and any associated proteins were immunoprecipitated using Anti-FLAG affinity gel (Sigma; A2220). Samples were washed 3 times with 0.5% NP-40 lysis buffer, then 3 times with 1X PBS to remove detergents, and immunoprecipitated complexes were eluted from beads using 3X FLAG peptide (Sigma; F4799). Eluates were TCA (trichloro-acetic acid)-precipitated and the resulting pellets trypsinized to generate peptides for analysis by liquid chromatography-mass spectrometry (LC-MS). MS spectra were used to identify eluted proteins, which were filtered using CRAPome and SAINT algorithms to remove in silico non-specific interactors, with a 1% False Discovery Rate (Mellacheruvu et al., 2013; Choi et al., 2011). Proteins with CRAPome scores of at least 2.0 and SAINT probability scores of at least 0.9 were selected as high confidence interactors of NLRP3.

Plasmid Cloning

pLX304 plasmids harboring the coding sequences for human CTP, ANT3, OGC, and Citrin with C-terminal V5 tags were acquired from the human ORFeome Collaboration (The ORFeome

Collaboration et al., 2016). These V5-tagged constructs, along with FLAG-tagged GFP were amplified and subcloned into the pEF expression vector. pEF plasmids containing coding sequences for FLAG-tagged or non-tagged human NLRP3, ASC, proIL-1β, and procaspase-1, along with the empty pEF vector, were kindly supplied by Dr. Michael Davis and Dr. Amina Negash. Using protein domain boundaries defined by UniProt (https://www.uniprot.org), truncated versions of the human NLRP3 and Citrin transcripts were amplified and subcloned into the pEF vector with C-terminal FLAG or V5 tags. Additionally, point mutations were introduced into full-length Citrin constructs to make them calcium-insensitive (E28A/N30A/D66A/T68A mutations) or transport-incapable (Q592R mutation) (Thangaratnarajah et al., 2014; Marmol et al., 2009; Wibom et al., 2009). PCR amplifications were performed using Phusion Hot Start II DNA Polymerase (Thermofisher; F549S). Amplified cDNA was subcloned into vectors using the In-Fusion HD cloning kit (TaKaRa; 638910). Cloned plasmids were propagated in DH5α competent cells (Thermofisher; 18265017), then extracted and purified using the ZymoPURE Plasmid Midiprep kit (Thermo Scientific; D4201). All cloned plasmids were verified by nucleotide sequencing using Genewiz (https://www.genewiz.com).

Plasmid Transfection

Unless specified otherwise, all plasmid transfections were performed using the Mirus Trans-IT LT1 transfection reagent (Mirus; MIR 2300), according to the manufacturer's instructions. In brief, HEK-293A or HEK-293T cells were seeded at 1.5x10^5 cells/well in 12-well plates, transfected when they attained ~70-80% confluency, then harvested 24-72 hours post-transfection. For reconstitution of NLRP3 inflammasomes in HEK-293A cells, 1 ng of ASC, 1 ng of procaspase-1, 100 ng of NLRP3 and 100 ng of proIL-1β plasmids were co-transfected with 800 ng of empty

vector, Citrin-V5, or ANT3-V5 plasmid in 12-well plates, with 1 mL medium/well. For other plate sizes, cell, medium, and transfection amounts were scaled proportionally.

CRISPR/Cas9 and ASC-mCherry cell lines

Citrin and ANT3 CRISPR gRNA sequences were designed using https://zlab.bio/guide-designresources, while NLRP3 and non-targeting gRNA sequences, as well as the pRRL-ASC-mCherry-Blast plasmid, were kindly provided by Dr. Michael Davis. gRNA sequences were inserted into the pRRL-empty-gRNA-Cas9-T2A-Puro vector (kindly provided by Dr. Dan Stetson; described by Eckard et al., 2014) using the In-Fusion HD cloning kit (TaKaRa; 638910). 3x10^6 HEK-293T cells/10 cm dish were transfected with 6 μg pRRL-gRNA-Cas9 or pRRL-ASC-mCherry plasmid, 3 μg pSPAX-2 packaging plasmid and 1.5 μg pMD2.G plasmid to generate lentiviruses. 24 hours post-transfection, DMEM medium was replaced with RPMI. 48 hours post-transfection, supernatants containing lentiviruses were filtered through 0.45 μm and used to infect THP-1 cells in the presence of 8 μg/mL Polybrene (Sigma Aldrich; TR-1003-G). THP-1 cells were cultured with lentiviruses 24 hours, washed with 1X PBS, then cultured 24 hours in fresh RPMI. Transduced THP-1 cells were selected with 5 μg/mL puromycin for 3-5 days and/or with 10 μg/mL blasticidin for 5-8 days, then cultured with regular RPMI after that. Knockout of CRISPR targets was confirmed by immunoblot. ASC-mCherry expression was verified by immunoblot and by stimuli-induced inflammasome speck formation, as measured by an Incucyte live-cell imager (Essen Biosciences). The following gRNA sequences were used to generate CRISPR knockout cell lines: NTC (non-targeting control gRNA): ACGGAGGCTAAGCGTCGCAA (Gray et al., 2016); NLRP3: TCTCTGTCTGACCCCTCGGG (Davis et al., 2019); ANT3: GCGGCCGTGGCTCCGATCGAG; and Citrin: GTCGAGTGACAAAGTCATTGG.

Immunoblot

Unless otherwise noted, cells were lysed in RIPA buffer (25 mM Tris-HCl pH 7.6, 150 mM NaCl, 1% NP-40, 1% sodium deoxycholate, 0.1% SDS), freshly supplemented with 250 μM okadaic acid, 1:100 protease inhibitor mixture (Sigma; P3340), and 1:1000 phosphatase inhibitor cocktail (Calbiochem; 524625). Lysate protein concentrations were quantified using a Bradford Protein Assay (BioRad; 5000201). Samples were diluted in RIPA, mixed with SDS-PAGE reducing sample buffer, and denatured for 5 minutes at 95°C. 10-20 μg lysate/well or 15 μL supernatant/well were separated on 4–20% TGX Precast Protein Gels (BioRad; 4561096) or 12% SDS-PAGE gels, then transferred onto polyvinylidene difluoride (PVDF) membranes (Fisher Scientific; IPVH00010). Membranes were blocked with 4% bovine serum albumin (BSA) diluted in 1X TBS buffer + 0.05% Tween-20 (TBST) for 1 hour at room temperature, then incubated 12-16 hours at 4°C with primary antibody diluted in blocking buffer. Membranes were then washed with TBST, incubated 1-3 hours at room temperature with HRP-conjugated secondary antibodies diluted in TBST, then washed again with TBST. To detect protein bands, membranes were treated with SuperSignal West Pico Chemiluminescent Substrate (ThermoFisher; 34578) and imaged using a BioRad ChemiDoc XRS+ System. Band densitometry and image processing were performed using BioRad Image Lab Software. The following primary antibodies were used: mouse anti-FLAG (1:1000; Sigma; F-1804), rabbit anti-FLAG (1:800; Sigma Aldrich; F7425), mouse anti-V5 (1:5000; ThermoFisher; R960-25), rabbit anti-V5 (1:5000; Abcam; Ab9116), mouse anti-α-tubulin (1:1000; Sigma; T6199), rabbit anti-NLRP3 (1:1000; CST; T6199), rabbit anti-caspase-1 p10 (1:1000; SCT; SC-515), rabbit anti-cleaved IL-1β (1:1000; CST; 83186S), rabbit anti-IL-1β (1:200; SCT; SC-7884), rabbit anti-ASC (1:1000; AG; AL-177), rabbit anti-ANT3 (1:2000; Abcam; ab154007), mouse anti-Citrin (1:500; SCT; SC-393303), Rabbit anti-Calnexin (1:1000;

CST; 2679), mouse anti-actin (1:1000; Millipore Sigma; MAB-1501). Secondary antibodies used: goat anti-rabbit HRP (1:10,000; Jackson ImmunoResearch; 111-035-003), goat anti-mouse HRP (1:10,000; Jackson ImmunoResearch; 115-035-003).

Co-Immunoprecipitation

Cells were lysed either in RIPA buffer (described above) or 1% NP-40 lysis buffer (50 mM Tris-HCl pH 7.6, 150 mM NaCl, 1% NP-40), supplemented with 250 μM okadaic acid, 1:100 protease inhibitor mixture (Sigma; P3340), and 1:1000 phosphatase inhibitor cocktail (Calbiochem; 524625). 150 μg lysate was then incubated at 4°C with magnetic protein G Dynabeads (Thermofisher; 10004D) pre-conjugated to mouse anti-FLAG antibody (1:200; Sigma; F-1804), mouse anti-V5 antibody (1:200; ThermoFisher; R960-25), or mouse IgG1 (1:200; ThermoFisher; 02-6100). After incubation, IP beads were washed 5 times with lysis buffer, at 5 minutes each wash, then eluted with 1X SDS-PAGE reducing sample buffer. IP eluates were transferred to new tubes, denatured 5 minutes at 95°C, then analyzed by immunoblot as described above.

Incucyte Cell Death Assays

THP-1 macrophages were seeded at 2x10^5 or 5x10^4 cells per well in 24-well or 96-well dishes, respectively. 48 hours after seeding, THP-1 macrophages were primed 4 hours with 5 ng/ml LPS, then mock-treated or treated with 10 μM Nigericin, 300 μg/μL MSU, or 2 μg/mL poly(dA:dT) to induce pyroptosis. Non LPS-primed THP-1 macrophages were treated with UV-inactivated HCV at MOI 0.1. To stimulate other cell death pathways, THP-1 macrophages were treated with 100 ng/ml TNFα and 10 μg/mL cycloheximide to induce apoptosis, or with 100 ng/ml TNFα, 50 μM zVAD, and 1 μM BV6 to induce necroptosis, as described previously (Gutierrez et al., 2017). All treatments were done in combination with 100 nM of cell-impermeable SYTOX-Green fluorescent

dye (Thermofisher; S7020) to quantify dead cells. Meanwhile, cells in separate wells were treated with 100 nM SYTO-Green dye (Thermofisher; S7559) to quantify total cells. Total and dead cells were quantified using an Incucyte ZOOM live-cell imager (Essen Bioscience), with 2-4 images acquired per well every 30 minutes–1 hour. For THP-1 macrophages stably expressing mCherry-tagged ASC, ASC specks were detected and quantified using the Incucyte red channel, while total number of SytO green-stained cells was quantified using the green channel. All treatments were done in duplicate or triplicate. Total cell death was calculated using mean SYTOX Green counts, while cell death percentage was calculated using the SYTOX-Green/SYTO-Green count ratios. Percent of cells with ASC specks was calculated as the number of ASC specks/total number cells in field of view.

IL-1β ELISA

Supernatants from treated THP-1 macrophages or HEK-293A cells were centrifuged 5 minutes at 10,000xg to remove cellular debris, transferred to a new tube, and stored at -80°C. After thawing, supernatants were assayed for the presence of IL-1β using a human IL-1β ELISA kit (BioLegend; 437004), according to the manufacturer's instructions. Absorbance at 450 nm and 570 nm was measured for each sample in triplicate using a spectrophotometer.

Cell Fractionation

Subcellular fractionation was performed as described previously (Bozidis et al., 2007). Briefly, THP-1 cells were resuspended in sucrose homogenization medium and broken up with a Dounce homogenizer. After pelleting nuclei and unbroken cells twice at 600xg, the supernatant was centrifuged three times at 10,400xg for 10 min to separate it into crude mitochondrial (MAM + mitochondria) and cytosol-microsomal fractions. Crude mitochondria were resuspended in buffer

Mannitol A, Dounce homogenized, and layered onto a 30% Percoll solution. After centrifuging this solution for 1 h at 95,000xg, MAM and mitochondrial fractions were harvested and washed with buffer Mannitol B. Microsomal and cytosolic fractions were then separated by centrifugation for 1 hour at 100,000xg, after which the cytosol fraction was concentrated using an Amicon Ultra-4 filter (Millipore Sigma; UFC810008). All membranous fractions were resuspended in 1% Triton lysis buffer (50 mM Tris-HCl, 150 mM NaCl, 1% Triton X-100, with freshly added protease and phosphatase inhibitors). Samples were subsequently analyzed by immunoblot as described above, loading ~2 μg fraction/well on SDS-PAGE gels.

Immunofluorescence Confocal Microscopy

HEK-293A cells were seeded at $7.5x10^4$ cells/well in 24-well plates containing 12mm glass coverslips pre-coated with Poly-L-lysine (Sigma; P4707). Once cells reached 70-80% confluence, they were transfected using Mirus Trans-IT LT1 reagent, as described above. 24-48 hours post-transfection, cells were washed with 1X PBS, then fixed with 4% paraformaldehyde (PFA) for 15-30 minutes at room temperature. Unless otherwise noted, PFA and all subsequent reagents were diluted in 1X PBS, and all steps were performed at room temperature. Fixed samples were washed with 10 mM glycine, permeabilized with 0.2% Triton X-100 for 5 minutes, then washed again with glycine solution. Permeabilized cells were blocked 1 hour with 3% BSA, then incubated 12-16 hours with primary antibodies diluted in blocking solution, with gentle rocking at 4°C. Samples were subsequently washed in 1X PBS, stained 1 hour with secondary antibodies and DAPI (ThermoFisher; D1306) diluted in blocking solution, then rinsed once more with 1X PBS. Coverslips containing stained cells were then briefly immersed in 100% EtOH, air dried, and mounted onto glass microscope slides with Prolong Gold Antifade Reagent (Life Technologies; P36934). Images were acquired with 40X and 60X oil immersion objectives on a Nikon Eclipse

Ti confocal microscope and processed using Nikon NIS-Elements Imaging Software. Inflammasome specks in HEK-293A cells were quantified as a percentage of total V5-expressing cells per field of view; seven random fields of view were selected per coverslip. The following antibodies were used: mouse anti-FLAG (1:100; Sigma; F-1804), rabbit anti-V5 (1:400; Abcam; Ab9116), mouse anti-TOM20 (1:250; Santa Cruz; SC-17764), goat anti-mouse IgG (H+L), Alexa Fluor 594 (1:600; ThermoFisher; A-11032), goat anti-mouse IgG (H+L), Alexa Fluor 488 (1:600; ThermoFisher; A-11029), goat anti-rabbit IgG (H+L), Alexa Fluor 594 (1:600; ThermoFisher; A-11037), and goat anti-rabbit IgG (H+L), Alexa Fluor 488 (1:600; ThermoFisher; A-11034).

Statistical Analysis

All statistical analyses were performed using GraphPad Prism Software, as described in the Figure legends.

2.5. Figures

A.

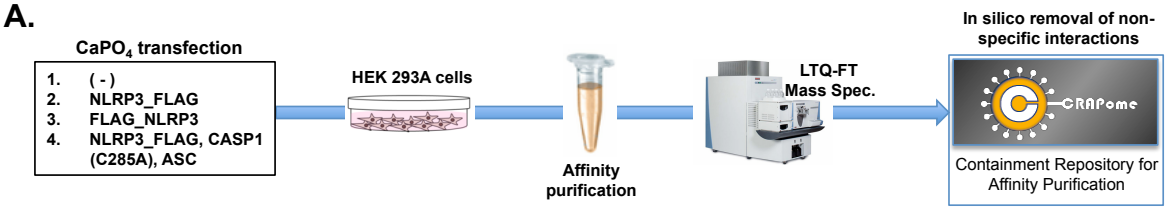

B.

	NLRP3_C-FLAG			NLRP3_N-FLAG			NLRP3_C-FLAG + ASC, CASP1		
Protein Name	**% Coverage**	**# PSMs**	**FC_B Score**	**% Coverage**	**# PSMs**	**FC_B Score**	**% Coverage**	**# PSMs**	**FC_B Score**
NLRP3	40.83	155	48.43	44.21	206	63.51	38.32	107	40.37
CASP1	0	0	0	0	0	0	22.72	7	3.36
ASC	0	0	0	0	0	0	37.78	9	3.69
SUGT1	21.92	7	3.28	21.62	5	2.51	32.6	11	5.01
NEK7	18.87	4	2.41	13.91	3	2.17	14.57	4	2.63
CTP (SLC25A1)	11.25	4	1.27	10.29	5	1.47	10.29	3	1.37
ANT3 (SLC25A6)	26.51	8	2.41	34.9	14	2.32	24.83	10	2.09
OGC (SLC25A11)	34.71	11	3.77	40.13	12	3.94	24.82	7	3.11
Citrin (SLC25A13)	17.48	12	4.46	14.37	11	4.52	18.07	10	5.16

C.

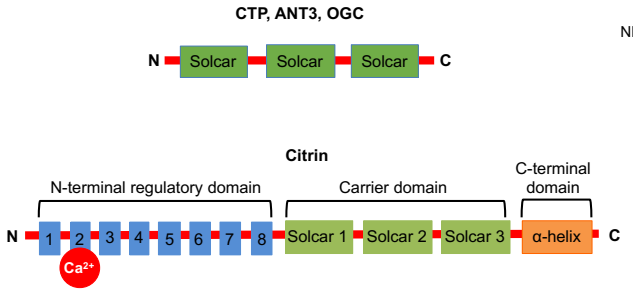

D.

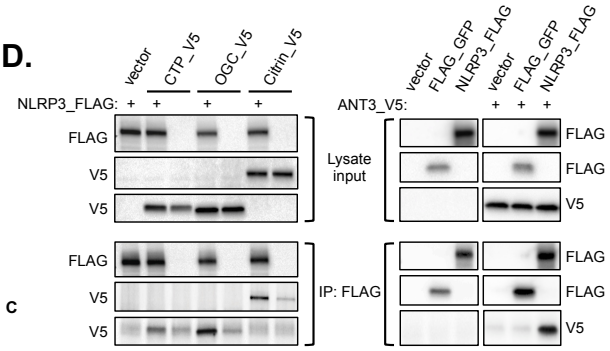

Figure 2.1. A proteomic link between mitochondrial SLC25 proteins and NLRP3

A. Schematic of affinity purification/mass spectrometry proteomics screen conducted to identify protein interactors of exogenously expressed FLAG-tagged NLRP3 in HEK-293A cells.

B. Mass spectrometry and CRAPome analyses of peptides mapping to the indicated proteins. These proteins were identified as high confidence interactors of NLRP3.

C. Schematic of CTP, ANT3, OGC, and Citrin protein domain structures. Citrin differs from the other three carriers in its extended N-terminal and C-terminal domains.

D. Coimmunoprecipitation of exogenous NLRP3-FLAG or GFP-FLAG (non-specific control) with indicated V5-tagged SLC25 proteins in HEK-293A cells; vector: empty plasmid.

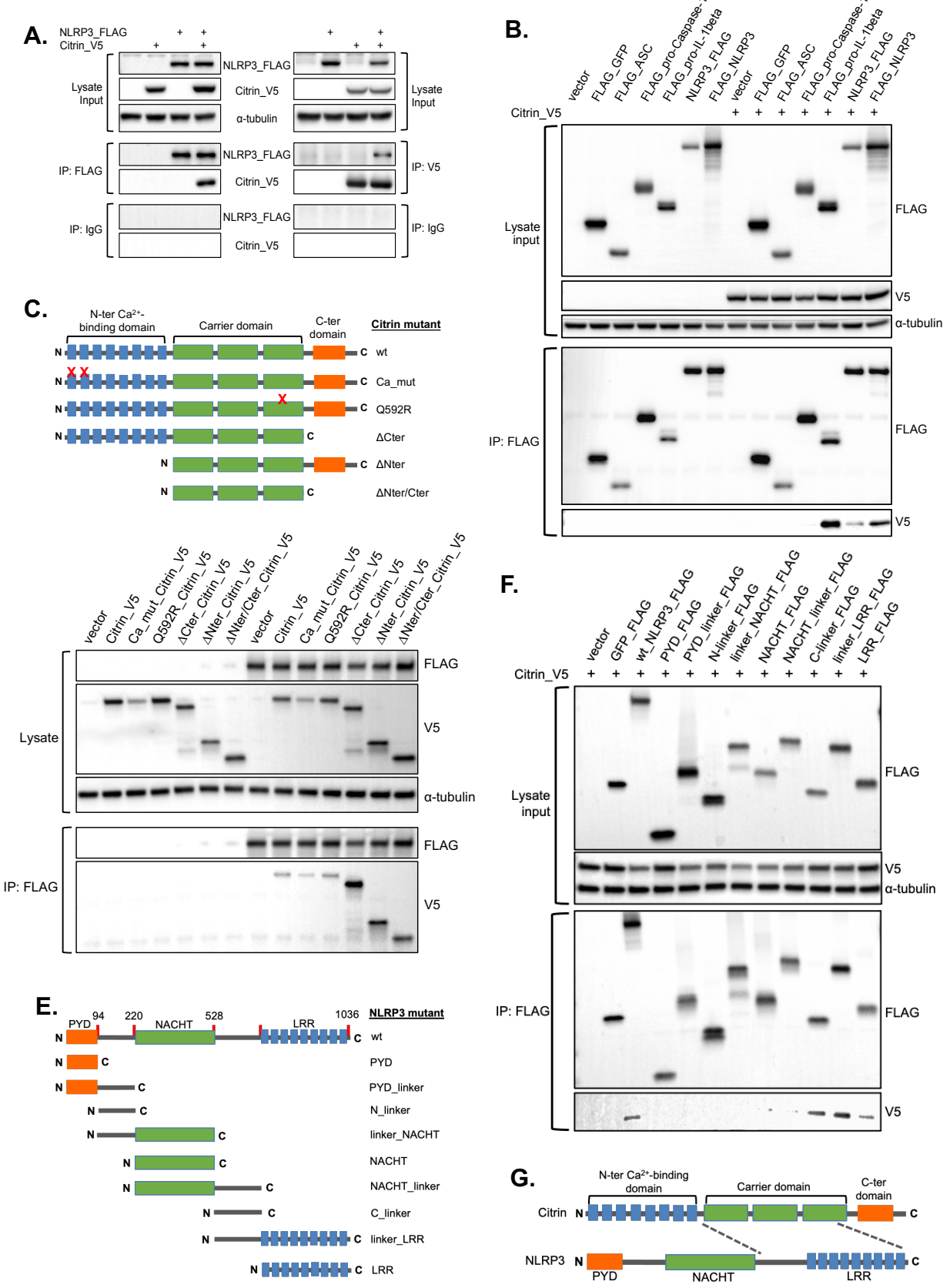
A.
NLRP3_FLAG
Citrin_V5
Lysate Input
IP: FLAG
IP: IgG
NLRP3_FLAG
Citrin_V5
α-tubulin
IP: V5
B.
vector
FLAG_GFP
FLAG_ASC
FLAG_pro-Caspase-1
FLAG_pro-IL-1beta
NLRP3_FLAG
FLAG_NLRP3
Citrin_V5
Lysate input
IP: FLAG
FLAG
V5
α-tubulin
C.
N-ter Ca²⁺-binding domain
Carrier domain
C-ter domain
Citrin mutant
wt
Ca_mut
Q592R
ΔCter
ΔNter
ΔNter/Cter
Lysate
IP: FLAG
F.
GFP_FLAG
wt_NLRP3_FLAG
PYD_FLAG
PYD_linker_FLAG
N-linker_FLAG
linker_NACHT_FLAG
NACHT_FLAG
NACHT_linker_FLAG
C-linker_FLAG
linker_LRR_FLAG
LRR_FLAG
E.
PYD
NACHT
LRR
94
220
528
1036
NLRP3 mutant
wt
PYD
PYD_linker
N_linker
linker_NACHT
NACHT
NACHT_linker
C_linker
linker_LRR
LRR
G.
Citrin
NLRP3

Figure 2.2. NLRP3 interacts with the solute carrier domain of Citrin

A. Coimmunoprecipitation of exogenously expressed FLAG-tagged NLRP3 with V5-tagged Citrin and vice versa from transfected HEK-293A cells; IgG: control immunoglobulin.

B. Coimmunoprecipitation of exogenous FLAG-tagged ASC, pro-Caspase-1, and proIL-1beta, N- and C-terminally FLAG-tagged NLRP3, and FLAG-tagged GFP (negative control) with V5-tagged Citrin in HEK-293A cells.

C. Schematic of Citrin mutants used for characterization of interaction with NLRP3. (wt: full-length human Citrin, Ca_mut: calcium insensitive mutant, Q592R: Citrin mutant lacking transport function, Δ: deletion of indicated protein domain)

D. Coimmunoprecipitation of exogenously expressed FLAG-tagged NLRP3 with indicated V5-tagged Citrin mutants in transfected HEK-293T cells.

E. Schematic of truncated NLRP3 mutants used for identification of binding domain with Citrin.

F. Coimmunoprecipitation of exogenous FLAG-tagged full-length and truncated NLRP3 with V5-tagged Citrin from transfected HEK-293T cells.

G. Diagram showing mapped interaction between NLRP3 LRR and Citrin solute carrier domains.

All immunoblot data are representative of at least three independent experiments.

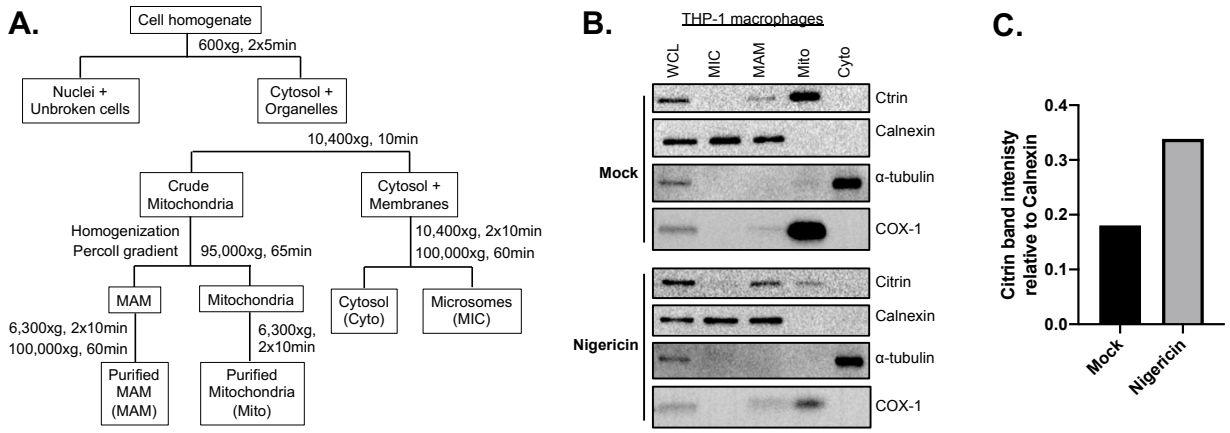

Figure 2.3. NLRP3 stimulation increases Citrin localization at the MAM

A. Fractionation schematic for separating THP-1 cell lysates into cytosol (Cyto), microsome (MIC), mitochondrial (Mito), and ER-mitochondria-associated membrane (MAM) fractions.

B. Immunoblot of indicated subcellular fractions from PMA-differentiated THP-1 macrophages that were mock-treated or stimulated with 10 μM Nigericin for 45 minutes. Calnexin is a marker of ER and MAM fractions, Cox-1 is a mitochondrial protein, while α-tubulin is cytosolic.

C. Densitometric analysis of Citrin band intensity relative to Calnexin in the MAM fraction.

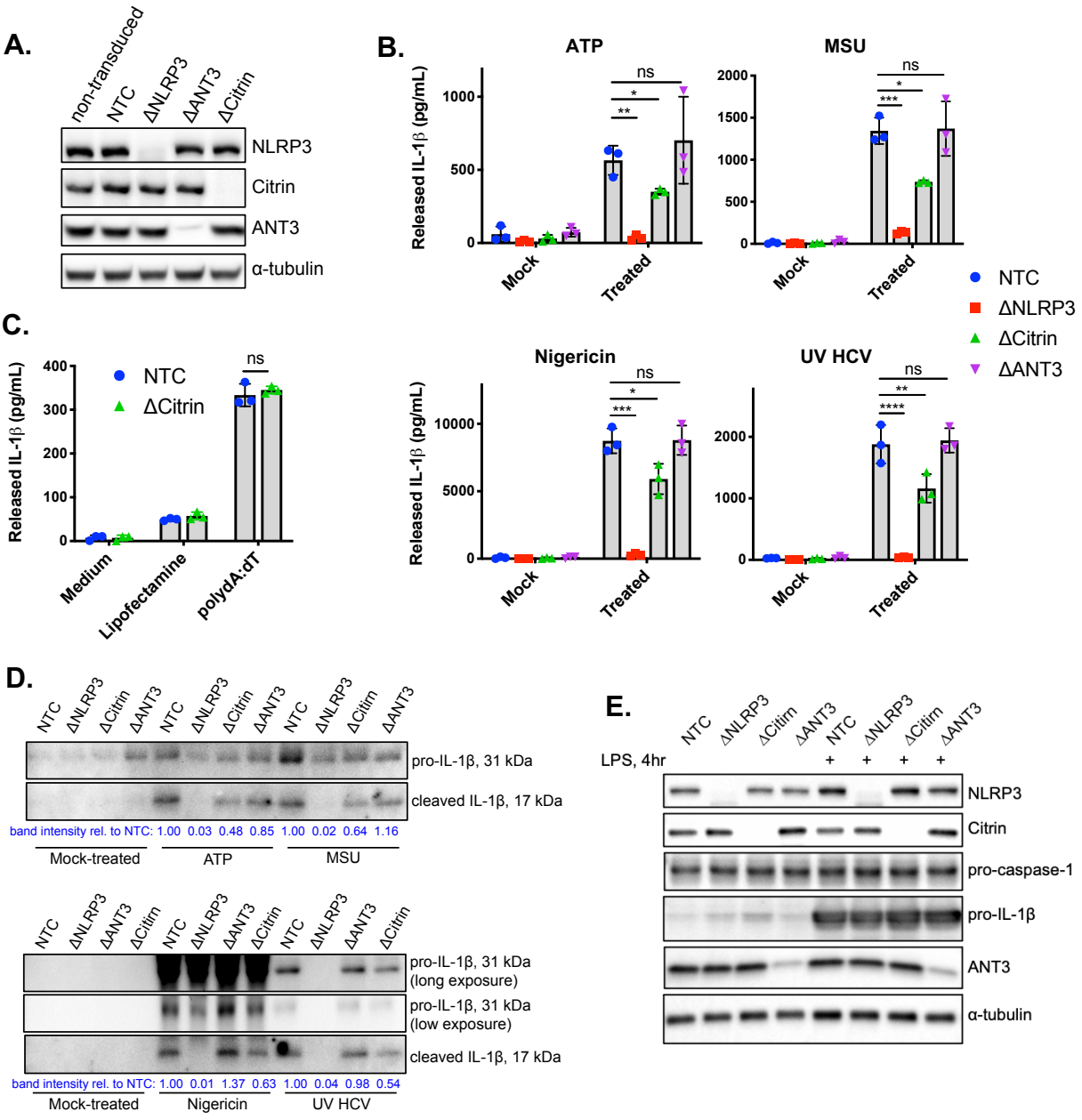
A.
non-transduced
NTC
ΔNLRP3
ΔANT3
ΔCitrin
NLRP3
Citrin
ANT3
α-tubulin
B.
ATP
MSU
Released IL-1β (pg/mL)
ns
*
**
***
Mock
Treated
NTC
ΔNLRP3
ΔCitrin
ΔANT3
C.
Medium
Lipofectamine
polydA:dT
Nigericin
UV HCV
****
D.
pro-IL-1β, 31 kDa
cleaved IL-1β, 17 kDa
band intensity rel. to NTC: 1.00 0.03 0.48 0.85 1.00 0.02 0.64 1.16
Mock-treated
ATP
MSU
pro-IL-1β, 31 kDa (long exposure)
pro-IL-1β, 31 kDa (low exposure)
band intensity rel. to NTC: 1.00 0.01 1.37 0.63 1.00 0.04 0.98 0.54
Nigericin
UV HCV
E.
LPS, 4hr
pro-caspase-1
pro-IL-1β

Figure 2.4. Citrin is required for optimal NLRP3-mediated IL-1β release in macrophages

A. Immunoblot analysis showing efficacy of CRISPR/Cas9 knockdown of NLRP3, ANT3, and Citrin in THP-1 cells. (wt: wild type parental cell line, NTC: THP-1 cells transduced with non-targeting control gRNA using CRISPR/Cas9, Δ: knockdown of specific protein using CRISPR/Cas9)

B. ELISA of IL-1β from supernatants of PMA-differentiated NTC, ΔNLRP3, ΔCitrin, and ΔANT3 THP-1 macrophages. Cells were primed 4 hr with 5 ng/mL LPS, then mock-treated with medium or treated 3 hr with 5 mM ATP, 300 μg/mL monosodium urate (MSU), or 10 μM nigericin. Non-primed cells were treated 3 hr with UV-inactivated hepatitis C virus at MOI 0.01. Data shown as mean with SD.

C. Immunoblots of non-cleaved (pro) and cleaved IL-1β detected in supernatants of PMA-differentiated THP-1 macrophages treated as in B. Cleaved IL-1β bands were quantified using densitometry, and the ratios of their intensities relative to the NTC band for each treatment are shown.

D. Immunoblot showing expression of inflammasome components NLRP3, procaspase-1, and proIL-1β in PMA-differentiated THP-1 macrophages primed 4 hr or not with 5 ng/mL LPS.

E. ELISA of IL-1β from supernatants of PMA-differentiated NTC and ΔCitrin THP-1 macrophages primed 4 hr with 5 ng/mL LPS, then treated 6 hr with medium, Lipofectamine transfection reagent, or transfected with 2 μg/mL poly(dA:dT). Data presented as mean with SD.

*All data are representative of at least three independent experiments. Statistical analyses were performed using one-way ANOVA with Dunnett's multiple comparisons test. $P \leq 0.05$, $^{**}P \leq 0.01$, $^{***}P \leq 0.001$ and $^{****}P \leq 0.0001$

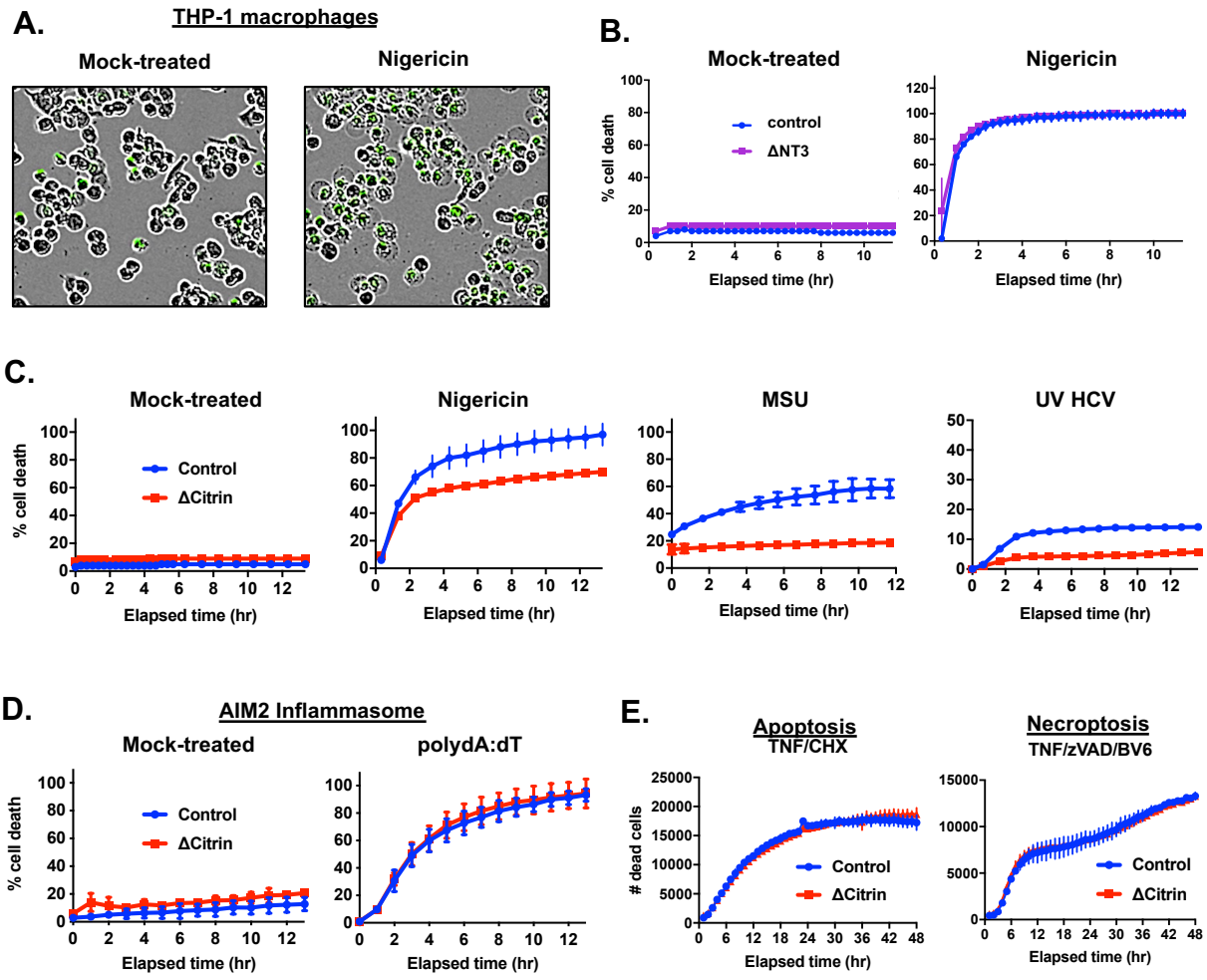

Figure 2.5. Citrin deletion suppresses NLRP3-mediated cell death

A. Live-cell images of PMA-differentiated THP-1 macrophages labeled with cell-impermeable SYTOX Green dye after 2 hr treatment with medium or 10 μM nigericin.

B. Cell death in control and ΔCitrin THP-1 macrophages mock-treated or treated with 10 μM nigericin, 300 μg/mL MSU, or UV-inactivated hepatitis C virus at MOI: 0.01, quantified as percentage of SYTOX Green-labeled cells relative to total cells.

C. Cell death in control and ΔANT3 THP-1 macrophages mock-treated or treated with 10 μM nigericin, quantified as in B.

D. Cell death in control and ΔCitrin THP-1 macrophages mock-treated or transfected with 2 μg/mL poly(dA:dT), quantified as in B.

E. Cell death in control and ΔCitrin THP-1 macrophages treated with TNFα and cyclohexamide to induce apoptosis, or with TNFα, zVAD, and BV6 to induce necroptosis, quantified as mean number of cells labeled with SYTOX Green dye/well.

*All data were acquired using an IncuCyte live cell imager and are representative of at least three independent experiments.

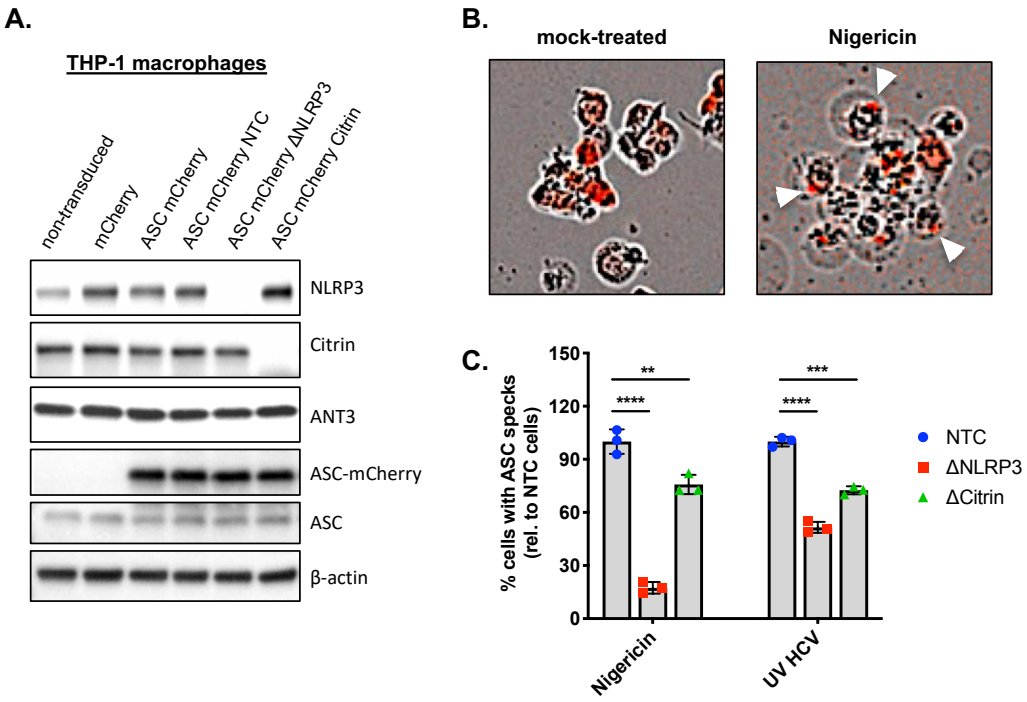

Figure 2.6. Citrin deletion reduces ASC speck formation

A. Immunoblot showing efficacy of CRISPR/Cas9 knockdown of NLRP3 and Citrin in THP-1 cells stably expressing mCherry-tagged ASC. (wt: "wild type" or non-transduced THP-1 cells, mCherry: THP-1 cells stably expressing mCherry, ASC mCherry: THP-1 cells stably expressing mCherry-tagged ASC, NTC: THP-1 cells transduced with non-targeting control gRNA using CRISPR/Cas9, Δ: knockdown of indicated protein using CRISPR/Cas9)

B. Live-cell images of PMA-differentiated THP-1 macrophages stably expressing mCherry-tagged ASC (labeled red). Right: Red ASC specks (marked by white arrows) formed inside cells following treatment with 10 μM nigericin.

C. Percentage of PMA-differentiated NTC, ΔNLRP3, and ΔCitrin THP-1 macrophages with ASC specks (relative to NTC cells) following stimulation with 10 μM nigericin or UV-inactivated hepatitis C virus (HCV) at MOI 0.01. Data presented as mean with SD and is representative of three replicate experiments. Statistical analyses were performed using one-way ANOVA with Dunnett's multiple comparisons test. $P \leq 0.05$, $^{**}P \leq 0.01$, $^{***}P \leq 0.001$ and $^{****}P \leq 0.0001$

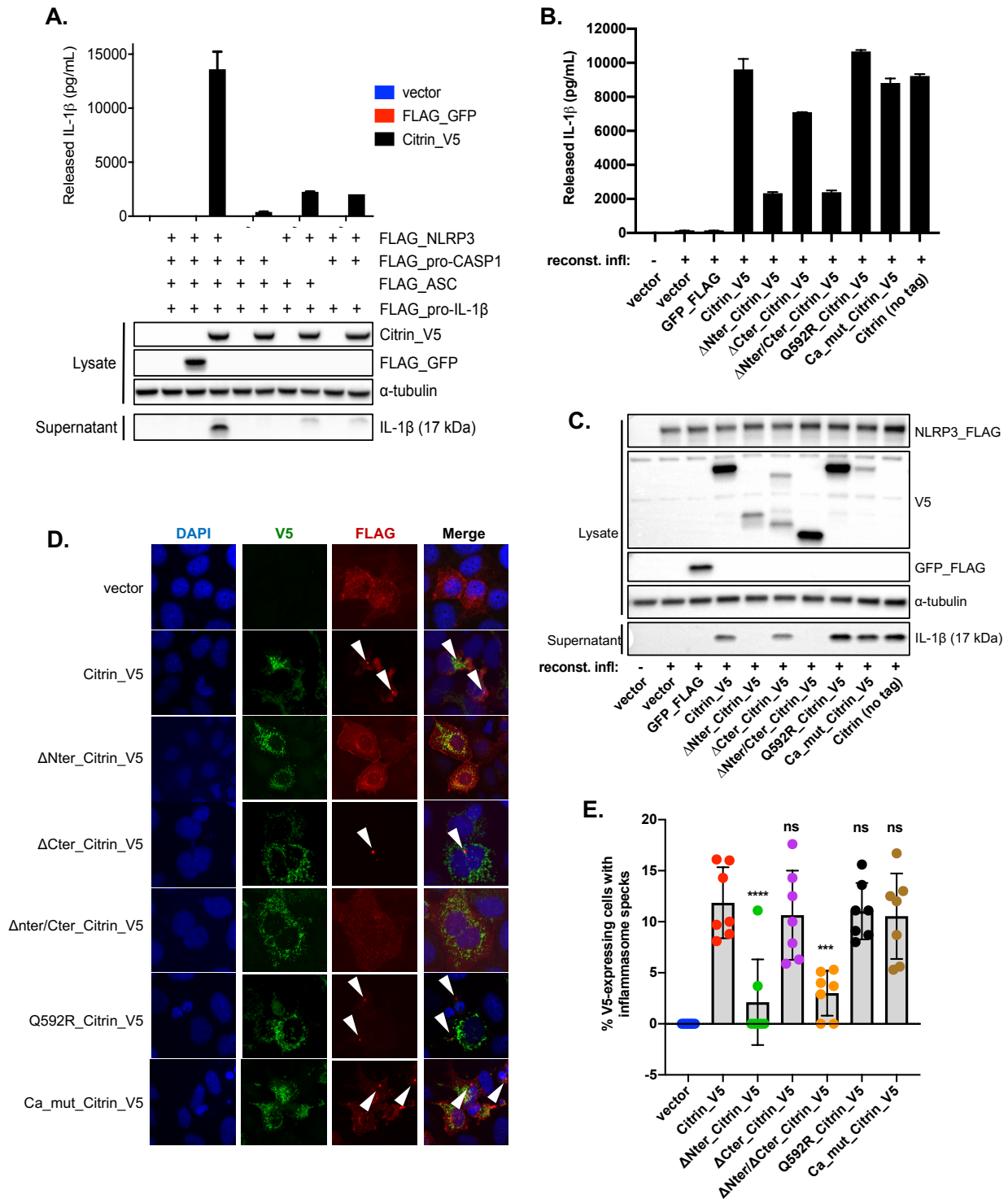

Figure 2.7. Overexpressed Citrin promotes NLRP3 inflammasome activation via its N-terminal domain

A. IL-1β ELISA of supernatants from HEK-293A cells harboring reconstituted NLPR3 inflammasomes (consisting of exogenously expressed FLAG-tagged NLRP3, ASC, procaspase-1, and proIL-1β in the indicated combinations), in which GFP-FLAG or V5-tagged Citrin was overexpressed and samples harvested 48 hr post plasmid transfection. Immunoblot analysis was performed on supernatants for cleaved IL-1β and cell lysates for the indicated targets.

B. IL-1β ELISA of supernatants from HEK-293A cells harboring reconstituted NLPR3 inflammasomes, in which GFP-FLAG or indicated V5-tagged Citrin mutants were overexpressed for 48 hr post plasmid transfection.

C. Immunoblot analysis of samples from Figure 6C, probing supernatants for cleaved IL-1β or cell lysates for the indicated targets.

D. Representative immunofluorescence microscopy images of HEK-293A cells harboring reconstituted NLPR3 inflammasomes, in which indicated V5-tagged Citrin mutants were overexpressed for 48 hr post plasmid transfection. V5 staining shown in green, FLAG in red, and DAPI in blue. White arrows indicate inflammasome specks.

E. Quantification of inflammasome specks from immunofluorescence microscopy images of HEK-293A cells harboring reconstituted NLPR3 inflammasomes, in which indicated V5-tagged Citrin mutants were overexpressed for 48 hr post plasmid transfection. Inflammasome specks were counted as a percentage of total V5-expressing cells within a field of view.

*Data from Figures 2.7A, 2.7B, and 2.7C are representative of at least three independent experiments, while data from Figures 2.7D and 2.7E are representative of two independent experiments. Statistical analyses were performed using one-way ANOVA with Dunnett's multiple comparisons test. $P \leq 0.05$, **$P \leq 0.01$, ***$P \leq 0.001$ and ****$P \leq 0.0001$

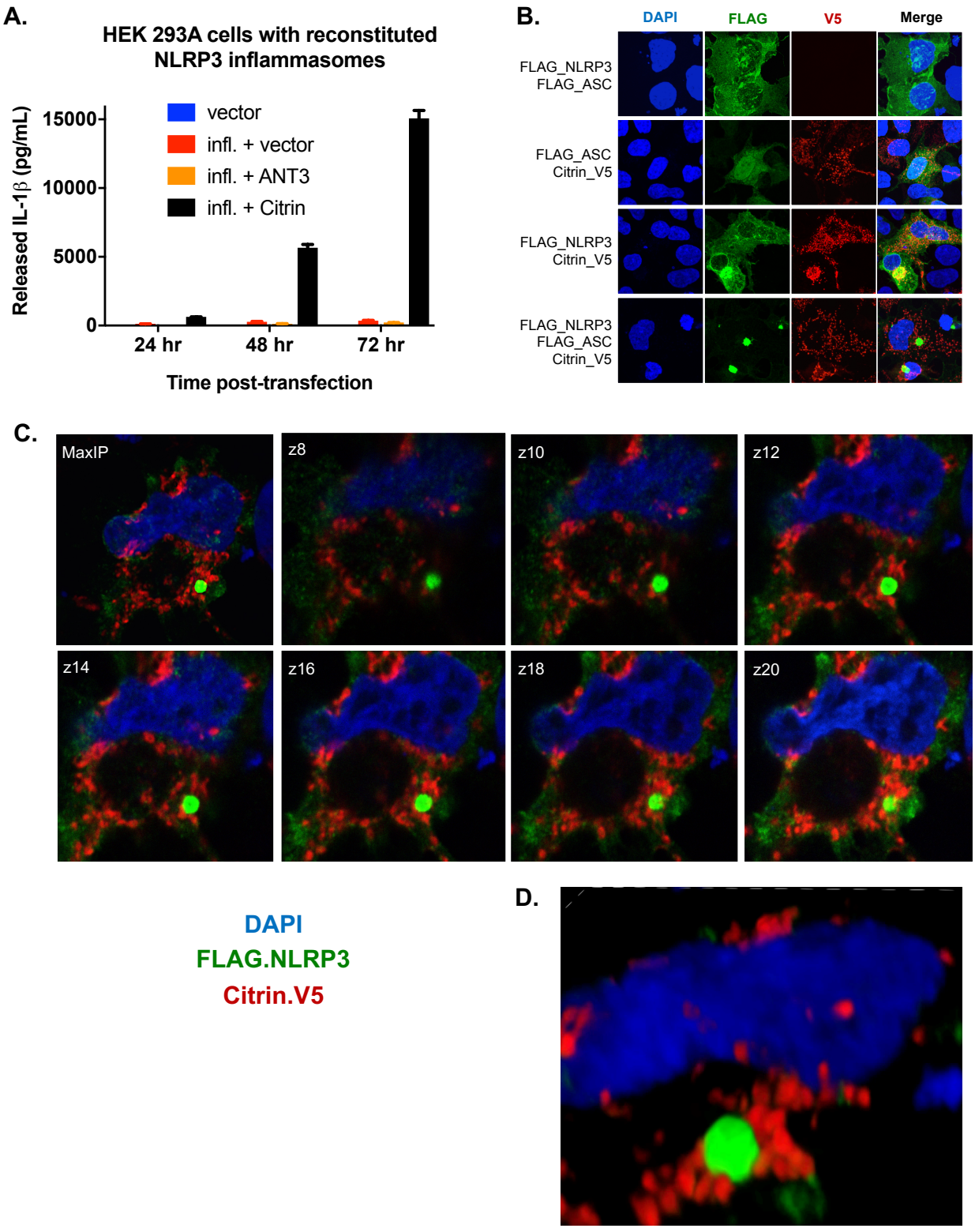
A.
HEK 293A cells with reconstituted NLRP3 inflammasomes
Released IL-1β (pg/mL)
15000
10000
5000
0
vector
infl. + vector
infl. + ANT3
infl. + Citrin
24 hr
48 hr
72 hr
Time post-transfection
B.
DAPI
FLAG
V5
Merge
FLAG_NLRP3
FLAG_ASC
FLAG_ASC
Citrin_V5
FLAG_NLRP3
Citrin_V5
FLAG_NLRP3
FLAG_ASC
Citrin_V5
C.
MaxIP
z8
z10
z12
z14
z16
z18
z20
DAPI
FLAG.NLRP3
Citrin.V5
D.

Figure 2.8. Overexpressed Citrin, but not ANT3, induces NLRP3 inflammasome speck formation and IL-1β release

A. IL-1β ELISA of supernatants from HEK-293A cells harboring reconstituted NLPR3 inflammasomes, in which GFP-FLAG, V5-tagged ANT3, or V5-tagged Citrin was overexpressed and supernatants harvested 24, 48, and 72 hr post plasmid transfection.

B. Immunofluorescence images of HEK-293A cells in which FLAG-NLRP3, FLAG-ASC, and Citrin-V5 were exogenously co-expressed in different combinations. V5 staining shown in red, FLAG in green, and DAPI in blue; 60X objective.

C. Immunofluorescence confocal images of HEK-293A cells transfected with plasmids encoding FLAG-NLRP3, FLAG-ASC, and Citrin-V5 showing Citrin-V5-stained mitochondria coming in close proximity to and "wrapping around" the NLRP3 inflammasome speck. Maximum intensity projection image (top left) and multiple z-planes of image presented. V5 staining shown in red, FLAG in green, and DAPI in blue; 60X objective.

D. Rotated three-dimensional image of inflammasome speck presented in Figure 2.8C, providing a closer view of the close association between the inflammasome speck and Citrin-V5-stained mitochondrial membranes. V5 staining shown in red, FLAG in green, and DAPI in blue; 60X objective.

*All data are representative of at least three independent experiments.

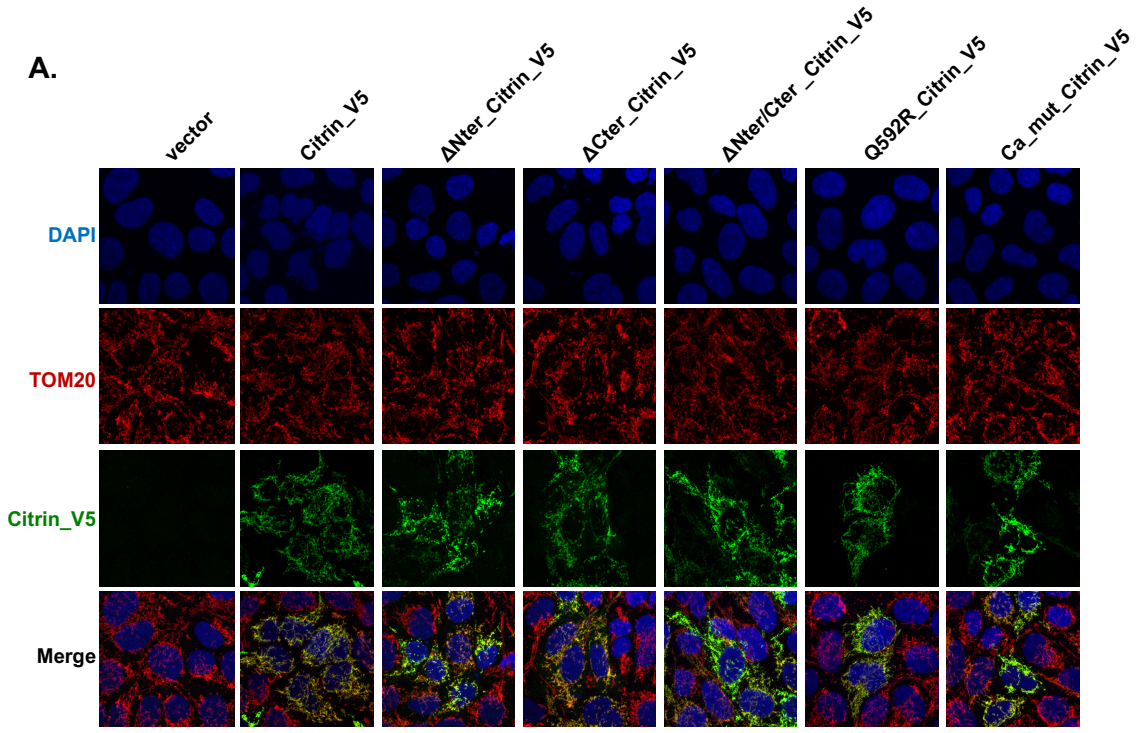

Figure 2.9. Overexpressed Citrin mutants co-localize with mitochondria.

Immunofluorescence images of HEK-293A cells exogenously overexpressing indicated V5-tagged Citrin mutants. Cells were co-stained for DAPI (blue), the mitochondrial marker TOM20 (red), and V5 (green). Images were acquired with a 60X objective and are representative of two independent experiments.

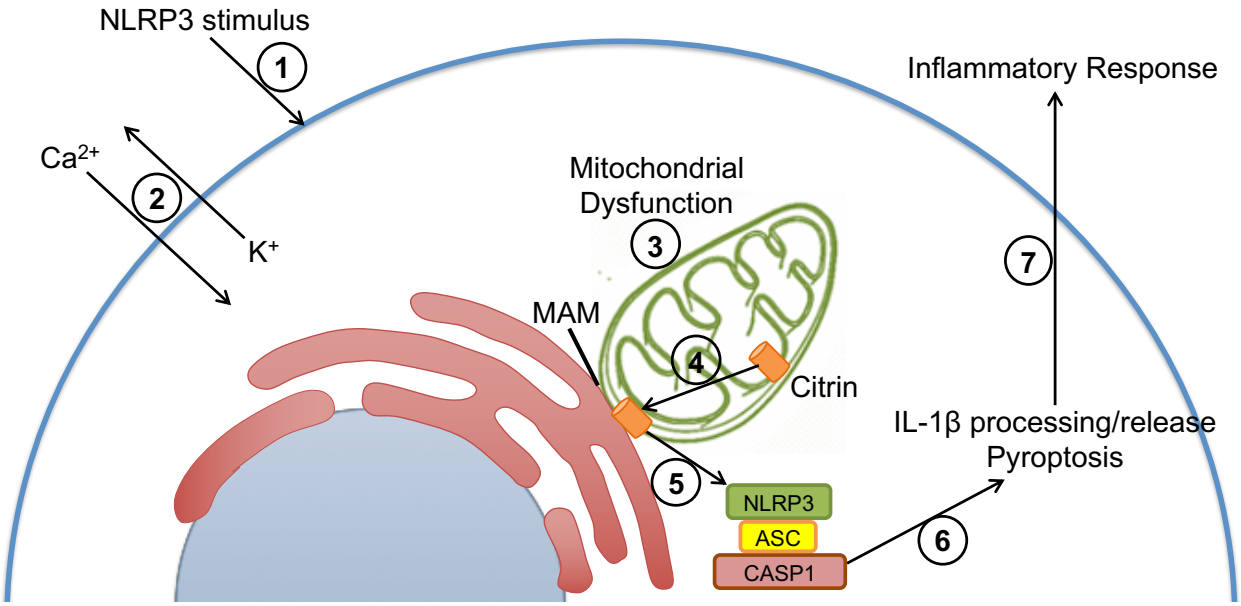

Figure 2.10. Proposed model for Citrin-mediated regulation of the NLRP3 inflammasome

Model figure depicting proposed mechanism for Citrin-mediated regulation of NLRP3 activation. Upon encountering an NLRP3 stimulus, a cell experiences multiple perturbations and disruptions, including K^+ efflux, Ca^{2+} influx, and mitochondrial dysfunction. In the context of this cellular stress, Citrin localization at the MAM increases, enabling it to interact with NLRP3 and promote NLRP3 inflammasome complex formation, the downstream results of which are release of proinflammatory cytokines and pyroptotic cell death.

2.6. Tables

GWAS Central query of study datasets which reported markers in listed genes or regions (no 5′ and no 3′ flanks) with -log p ≥ 1						
Phenotype	**NLRP3**	**NEK7**	**Citrin (SLC25A13)**	**OGC (SLC25A11)**	**ANT3 (SLC25A6)**	**CTP (SLC25A1)**
4 kHz hearing threshold	+		+			
Adult height	+					
Age-related macular degeneration	+	+	+			
Alzheimer's disease	+		+			
Amyotrophic lateral sclerosis	+		+			
Anti-cyclic citrullinated peptide-positive rheumatoid arthritis		+				
Asthma	+	+	+			
Birth weight			+			
Bipolar disorder	+	+				
Body mass index	+	+	+			
Brain glutamate concentrations		+	+			
Breast cancer		+				
C-reactive protein level	+					
Crohn's disease	+		+			
Diabetic nephropathy in type I diabetes			+			
Fasting glucose-related: fasting plasma glucose	+	+				
Fasting glucose-related: homeostatic model assessment of beta-cell function		+	+			
Fasting insulin-related: fasting insulin	+	+	+			
Fasting insulin-related: homeostatic model assessment of insulin resistance	+	+	+			
Fibrinogen	+					
Flucloxacillin-induced liver injury	+	+		+		
Glycated hemoglobin levels			+			
Height			+			
Height-adjusted highest forced expiratory volume		+	+			
Ischemic stroke			+			
Log10 fibrinogen		+	+			
Log10 glycosylated haemoglobin	+	+	+			
Narcolepsy		+	+			
Nephropathy			+			
Nicotine dependence, gender-differentiated		+				
Parkinson's disease	+	+	+			
Partial epilepsies		+	+			
Proinsulin levels	+	+	+			
Prostate cancer		+	+			
Psoriasis	+	+				
Response to antipsychotic therapy, extrapyramidal side effects: abnormal involuntary movement scale	+					
Rheumatoid arthritis		+				
Schizophrenia	+	+	+			
Serum cholesterol		+	+			
Systolic blood presure	+	+				
Two-hour glucose challenge	+					
Type II diabetes	+	+	+			
Ulcerative colitis	+	+	+	+		

Key

Citrin and NLRP3

Citrin and NEK7

Citrin, NLRP3, and NEK7

Table 2.1. Citrin is associated with metabolic and inflammatory disorders

Results of a query of genome-wide association study datasets that reported markers in the indicated genes (SLC25A1, SLC25A6, SLC25A11, SLC25A13, NEK7, and NLRP3) with –log p ≥ 1. Phenotypes associated with these genes are indicated with + signs. Overlapping phenotype associations between NLRP3, NEK7, and/or SLC25A13 (Citrin) are indicated by color, as described in the Key. Query was performed using GWAS Central (www.gwascentral.org).

3. Conclusions and Future Directions

In 2013, through the work of mutliple groups, it was discovered that mitochondrial MAVS, Mitofusin-2, and cardiolipin recruited NLPR3 to mitochondrial membranes and promoted its inflammasome activity (Subramanian et al. 2013, Park et al., 2013; Ichinohe et al., 2013; Iyer et al., 2013). Several years later, it was observed that NLRP3 was trafficked to mitochondrial membranes along with procaspase-1 during inflammasome priming (Elliott et al., 2018). During the same time, through the work of two separate teams, it was uncovered that MAM and mitochondria-bound NLRP3 was trafficked toward the Golgi, where activating signals triggered its release from mitochondria and induced its association with the dissociated *trans*-Golgi network (Zhang et al., 2017; Chen and Chen, 2018). While definitive proof is still needed, accumulating evidence indicates that this perinuclear region where close mitochondria-Golgi contacts occur serves as the nucleation site for the NLRP3 inflammasome. Building on this mechanistic understanding of NLRP3 trafficking and activation, here we present evidence for another mitochondrial interactor of NLRP3 - Citrin. We postulate that Citrin works together with MAVS, Mitofusin-2, and/or cardiolipin to create a molecular scaffold that facilitates NLPR3 localization to mitochondria and MAM membranes, promoting downstream nucleation of the inflammasome complex.

Our findings that Citrin knockout partially suppressed NLRP3 inflammasome activity in THP-1 macrophages (**Figures 2.4, 2.5, and 2.6**), while Citrin overexpression induced NLRP3 inflammasome complex formation in cells with reconstituted NLRP3 inflammasomes (**Figure 2.7**), support the model described above. The inability of Citrin deletion to completely ablate NLRP3 inflammasome activity in THP-1 cells may reflect Citrin's shared role with other scaffolding proteins and cardiolipin to recruit NLRP3 to mitochondrial and MAM membranes.

Thus, while Citrin deletion may lower the efficiency of NLPR3 trafficking to these subcellular sites, Citrin's absence may not completely impede it. In the context of Citrin overexpression, it is possible that Citrin is driven to localize at subcellular compartments outside the IMM, thereby enabling its interaction with NLRP3 and promoting subsequent NLRP3 aggregation and nucleation of the inflammasome complex. Further investigations are needed to elucidate how Citrin's subcellular localization is affected by its overexpression.

Our observation that Citrin localization increased in the MAM fraction of PMA-differentiated THP-1 macrophages following nigericin treatment was intriguing (**Figure 2.3**). Previous studies have reported increased localization of NLRP3 at MAM membranes following inflammasome stimulation (Zhou et al., 2011; Zhang et al., 2017), while others have reported trafficking of mitochondrial carriers, including Citrin, between MAM and mitochondrial subcellular fractions during RNA virus infection (Horner et al., 2015). Of course, higher resolution interaction studies will be needed to definitively ascertain that the MAM is the subcellular location where the NLRP3-Citrin interaction takes place. More studies are also needed to uncover whether or not Citrin associates with other MAM proteins, such as Mitofusin-2 or MAVS, in response to NLRP3 stimuli.

The mechanism by which Citrin, an inner mitochondrial membrane protein, comes into contact with NLRP3, which is cytoplasmic, ER-bound, or associated with the outer mitochondrial membrane (OMM), presents a puzzle. It is tempting to speculate that exposure of an IMM protein like Citrin effectively presents an intracellular DAMP that is detected by the sensor protein, NLRP3. After all, under normal cellular conditions, these two proteins should never come into contact with each other. Inflammasome priming and activation-induced translocation of cardiolipin from the IMM to OMM (Iyer et al., 2013; Elliot et al., 2018) presents a possible route

for Citrin movement to the OMM. Reconstitution of many mitochondrial carriers into liposomes requires cardiolipin, revealing it to be a necessary lipid for proper folding and IMM integration of many MCs (Palmieri and Monne, 2016). It would therefore be informative to investigate whether or not cardiolipin translocation to the OMM promotes a similar OMM relocation by Citrin.

While we focused our studies on Citrin-mediated regulation of NLRP3, the role of its homologue, Aralar, remains to be explored. Aralar was not identified as a high confidence interactor of NLRP3 in our proteomics screen performed using HEK-293A cells, though this does not necessarily preclude its ability to interact with NLRP3, which warrants further investigation. It certainly would be interesting if human Citrin interacted with NLPR3, while Aralar did not. After all, Aralar and Citrin are very similar in structure and function. The two proteins share 77% amino acid sequence similarity, have EF-hand-containing N-terminal domains and a regulatory C-terminal domain, bind a single Ca^{2+} ion, and transport aspartate/glutamate across the IMM (del Arco et al., 2000; Palmieri et al., 2001, Thangaratnarajah et al., 2014). Recently, Aralar was linked to MAVS innate immune signaling in HEK-293 cells. Challenging these cells with transfected poly(I:C) or Sendai virus infection upregulated the microRNAs miR-302b and miR-372, which reduced Aralar expression, resulting in decreased cellular NADH levels and attenuation of the MAVS-interferon signaling pathway (Yasukawa et al., 2020). Surprisingly, Aralar was also found to associate with MAVS through the mitochondrial prohibitin complex (Yasukawa et al., 2020). Given this connection between Aralar and innate immune signaling, an exploration of Aralar's role in molecular regulation of the NLRP3 inflammasome and potential complementation of Citrin function would be informative. These questions could best be addressed using Aralar knockout and Aralar/Citrin double knockout macrophage cell models.

Here we present evidence that overexpressed Citrin induced NLRP3 speck formation and NLRP3-dependent IL-1β release in HEK-293A cells with reconstituted NLRP3 inflammasomes (**Figures 2.7 and 2.8**). Intriguingly this Citrin-mediated promotion of NLRP3 activity was dependent on its N-terminal domain, but not its calcium-binding or solute transport functions, since Citrin mutants that could not bind calcium or transport solutes still induced inflammasome activity (**Figure 2.7B and 2.7E**). These Citrin mutants contained well-characterized amino acid substitutions reported to inhibit calcium responsiveness (E28A/N30A/D66A/T68A mutant) or prevent solute transport (Q592R mutant) without affecting mitochondrial localization (Wibom et al., 2009; Marmol et al., 2009; Thangaratnarajah et al., 2014). Still, a role for mitochondrial metabolism in Citrin-mediated regulation of NLRP3 inflammasome activity cannot be discounted. Citrin's carrier function is to exchange mitochondrial aspartate for cytoplasmic glutamate and a proton; this allows transfer of NADH reducing equivalents from the cytosol to mitochondria (Palmieri et al., 2001). Citrin plays a critical role in the malate/aspartate NADH shuttle (MAS), which helps maintain a healthy cellular [NAD^+]/[NADH] ratio (Amoedo et al., 2016). Increased cytosolic calcium concentrations and Citrin overexpression have been shown to greatly increase MAS activity (Palmieri et al., 2001). Citrin knockout, meanwhile, abrogated aspartate transport and MAS activity in liver cells (Sinasac et al., 2004). While Aralar can compensate for lack of Citrin in skeletal and heart muscles cells (Contreras et al., 2007), the impact of Citrin loss on mitochondrial function in immune cells, as well as Aralar's ability to compensate for Citrin absence, remain open questions. NLRP3 sensitivity to both cellular [NAD^+]/[NADH] ratios and disruptions in glycolysis (Sanman et al., 2016; Prochniki and Latz, 2017) offer possible avenues by which Citrin-mediated changes to mitochondrial function can regulate NLRP3 activity. Thus, the effect of Citrin deletion or overexpression on mitochondrial function in macrophages should

be investigated further. Specifically, the role of the MAS pathway in NLRP3 regulation warrants a closer look, both through pharmacological inhibition of MAS and through deletion of OGC, the 2-oxoglutarate/malate carrier, which, together with Citrin/Aralar, also plays a critical transport role in the MAS pathway (Amoedo et al., 2016).

Finally, while our research demonstrated a role for Citrin-mediated NLRP3 regulation *in vitro*, recapitulating these findings *in vivo* would help further establish biological relevance. In 2004, Sinasac, et al. generated Citrin knockout mice to establish a mouse model for adult-onset type II citrullinemia (CTLN2), a liver disease caused by Citrin deficiency in humans. Hepatocytes from Citrin ko mice exhibited impaired MAS activity, gluconeogenesis, and ureogenesis, but did not recapitulate the CTLN2 phenotype observed in humans, which is characterized by loss of arginosuccinate synthetase (ASS) activity (Sinasac et al., 2004). In mice, unlike in humans, mitochondrial glycerol 3-phosphate dehydrogenase (mGPD) maintains normal ASS levels when Citrin is absent (Sinasac et al., 2004). Confirming this, mGPD/Citrin double knockout mice exhibited disease pathology closely resembling that of human CTLN2 (Saheki et al., 2007). To our knowledge, however, experiments involving inflammatory disease models that engage NLRP3 have not yet been reported for Citrin knockout or mGPD/Citrin double knockout mice. Therefore, challenging Citrin knockout mice with viral or chemical stimuli that engage the NLRP3 inflammasome and measuring resulting inflammatory responses would help determine whether or not Citrin plays a role in regulating inflammation *in vivo*. Additionally, testing NLRP3 inflammasome responses in peripheral blood monocytes (PBMCs) from Citrin-deficient human donors and comparing them to those of healthy donors would also provide valuable insights into the human clinical relevance of Citrin-mediated NLPR3 inflammasome control.

4. References

Amoedo, N.D., Punzi, G., Obre, E., Lacombe, D., De Grassi, A., Pierri, C.L., and Rossignol, R. (2016). AGC1/2, the mitochondrial aspartate-glutamate carriers. Biochimica et Biophysica Acta *1863*, 2394-2412.

Barry, R., John, S.W., Liccardi, G., Tenev, T., Jaco, I., Chen, C-H., Choi, J., Kasperkiewicz, P., Fernandes-Alnemri, T., Alnemri, E., et al. (2018). SUMO-mediated regulation of NLRP3 modulates inflammasome activity. Nat. Commun. *9,* 3001.

Bauernfeind, F.G., Horvath, G., Stutz, A., Alnemri, A.S., MacDonald, K., Speert, D., Fernandes-Alnemri, T., Wu, J., Monks, B.G., Fitzgerald, K.A., et al. (2009). Cutting Edge: NF-κB Activating Pattern Recognition and Cytokine Receptors License NLRP3 Inflammasome Activation by Regulating NLRP3 Expression. J. Immun. *183*, 787-791.

Beck, T., Shorter, T., and Brookes, A.J. (2020). GWAS Central: a comprehensive resource for the discovery and comparison of genotype and phenotype data from genome-wide association studies. Nucleic Acids Res. *48*, D933-D940. https://www.gwascentral.org

Boucher, D., Monteleone, M., Coll, R. C., Chen, K. W., Ross, C. M., Teo, J. L., Gomez, G. A., Holley, C. L., Bierschenk, D., Stacey, K. J., et al. (2018). Caspase-1 self-cleavage is an intrinsic mechanism to terminate inflammasome activity. J. Exp. Med. *215*(3), 827–840.

Bozidis, P., Williamson, C.D., and Colberg-Poley, A.M. (2007). Isolation of Endoplasmic Reticulum, Mitochondria, and Mitochondria-Associated Membrane Fractions from Transfected Cells and from Human Cytomegalovirus-Infected Primary Fibroblasts. Current Protoc. Cell Biol. *37*, 3.27.1-3.27.23.

Bruchard, M., Rebé, C., Derangère, V., Togbé, D., Ryffel, B., Boidot, R., Humblin, E., Hamman, A., Chalmin, F., Berger, H., et al. (2015). The receptor NLRP3 is a transcriptional regulator of TH2 differentiation. Nat. Immunol. *16,* 859–870.

Chen, J. and Chen, Z.J. (2018). PtdIns4P on dispersed trans-Golgi network mediates NLRP3 inflammasome activation. Nature *564*, 71-76.

Chevriaux, A., Pilot, T., Derangère, V., Simonin, H., Martine, P., Chalmin, F., Ghiringhelli, F., and Rébé, C. (2020). Cathepsin B Is Required for NLRP3 Inflammasome Activation in Macrophages, Through NLRP3 Interaction. Front. Cell Dev. Biol. *8,* 167.

Choi, H., Larsen, B., Lin, Z-Y., Breitkreutz, A., Mellacheruvu, D., Fermin, D., Qin, Z.S., Tyers, M., Gingras, A-C., and Nesvizhskii, A.I. (2011). SAINT: probabilistic scoring of affinity purification–mass spectrometry data. Nat. Methods *8,* 70–73. http://saint-apms.sourceforge.net/Main.html

Clémençon, B., Babot, M., and Trézéguet, V. (2013). The mitochondrial ADP/ATP carrier (SLC25 family): Pathological implications of its dysfunction. Mol. Aspects Med. *34*, 485-493.

Contreras, L., Gomez-Puertas, P., Iijima, M., Kobayashi, K., Saheki, T., and Satrústegui, J. (2007). Ca^{2+} Activation Kinetics of the Two Aspartate-Glutamate Mitochondrial Carriers, Aralar and Citrin: role in the heart malate-aspartate NADH shuttle. J. Biol. Chem. *282*, 7098 –7106.

Davis, M.A., Fairgrieve, M.R., Hartigh, A.D., Yakovenko, O., Duvvuri, B., Lood, C., Thomas, W.E., Fink, S.L., and Gale Jr, M. (2019). Calpain drives pyroptotic vimentin cleavage, intermediate filament loss, and cell rupture that mediates immunostimulation. Proc. Natl. Acad. Sci. USA *116,* 5061-5070.

Del Arco, A. and Satrústegui, J. (1998). Molecular Cloning of Aralar, a New Member of the Mitochondrial Carrier Superfamily That Binds Calcium and Is Present in Human Muscle and Brain. J. Biol. Chem. *273,* 23327-23334.

Del Arco, A., Agudo, M., and Satrústegui, J. (2000). Characterization of a second member of the subfamily of calcium-binding mitochondrial carriers expressed in human non-excitable tissues. Biochem. J. *345,* 725-732.

Di, A., Xiong, S., Ye, Z., Malireddi, R.K.S., Kometani, S., Zhong, M., Mittal, M., Hong, Z., Kanneganti, T.D., Rehman, J., et al. (2018). The TWIK2 Potassium Efflux Channel in Macrophages Mediates NLRP3 Inflammasome-Induced Inflammation. Immunity *49,* 56-65.

Dinarello, C.A. (2009). Immunological and Inflammatory Functions of the Interleukin-1 Family. Ann. Rev. Immunol. *27*, 519-550.

Ding, J., Wang, K., Liu, W., She, Y., Sun, Q., Shi, J., Sun, H., Wang, D-C., and Shao, F. (2016). Pore-forming activity and structural autoinhibition of the gasdermin family. Nature *535,* 111–116.

Dostert, C., Petrilli, V., Van Bruggen, R., Steele, C., Mossman, B.T., and Tschopp, J. (2008). Innate immune activation through Nalp3 inflammasome sensing of asbestos and silica. Science *320*, 674–677.

Duncan, J. A., Bergstralh, D. T., Wang, Y., Willingham, S. B., Ye, Z., Zimmermann, A. G., and Ting, J. P. Y. (2007). Cryopyrin/NALP3 binds ATP/dATP, is an ATPase, and requires ATP binding to mediate inflammatory signaling. Proc. Natl. Acad. Sci. USA *104,* 8041–8046.

Eckard, S.C., Rice, G.I., Fabre, A., Badens, C., Gray, E.E., Hartley, J.L., Crow, Y.J., and Stetson, D.B. (2014). The SKIV2L RNA exosome limits activation of the RIG-I-like receptors. Nat. Immunol. *15,* 839-45.

Elliott, E.I., Miller, A.N., Banoth, B., Iyer, S.S., Stotland, A., Weiss, J.P., Gottlieb, R.A., Sutterwala, F.S., and Cassel, S.L. (2018). Cutting Edge: Mitochondrial Assembly of the NLRP3 Inflammasome Complex Is Initiated at Priming. J. Immunol. *200*, 3047-3052.

Ferramosca, A., and Zara, V. (2013). Biogenesis of mitochondrial carrier proteins: Molecular mechanisms of import into mitochondria. Biochimica et Biophysica Acta *1833,* 494-502.

Franchi, L., Eigenbrod, T., and Núñez, G. (2009). Cutting Edge: TNF-α Mediates Sensitization to ATP and Silica via the NLRP3 Inflammasome in the Absence of Microbial Stimulation. J. Immunol. *183*, 792-796.

Franchi, L., Eigenbrod, T., Muñoz-Planillo, R., Ozkurede, U., Kim, Y-G., Chakrabarti, A., Gale Jr., M., Silverman, R.H., Colonna, M., Akira, S., et al. (2014). Cytosolic Double-Stranded RNA Activates the NLRP3 Inflammasome via MAVS-Induced Membrane Permeabilization and K^+ Efflux. J. Immunol. *193,* 4214-4222.

Gray, E.E., Winship, D., Snyder, J.M., Child, S.J., Geballe, A.P., and Stetson, D.B. (2016). The AIM2-like Receptors Are Dispensable for the Interferon Response to Intracellular DNA. Immunity *45,* 255-266.

Groß, C. J., Mishra, R., Schneider, K. S., Médard, G., Wettmarshausen, J., Dittlein, D. C., Shi, H., Gorka, O., Koenig, P-A., Fromm, S., et al. (2016). K^+ Efflux-Independent NLRP3 Inflammasome Activation by Small Molecules Targeting Mitochondria. Immunity *45,* 761-773.

Guo, W., Liu, W., Chen, Z., Gu, Y., Peng, S., Shen, L., Shen, Y., Wang, X.,Feng, G.-S., Sun, Y., et al. (2017). Tyrosine phosphatase SHP2 negatively regulates NLRP3 inflammasome activation via ANT1-dependent mitochondrial homeostasis. Nat. Comm. *8*, 2168.

Gurung, P., Lukens, J.R., and Kanneganti, T.D. (2015). Mitochondria: diversity in the regulation of the NLRP3 inflammasome. Trends in Mol. Med. *21*: 193-201.

Gutierrez, K.D., Davis, M.A., Daniels, B.P., Olsen, T.M., Ralli-Jain, P., Tait, S.W., Gale, M.Jr. Oberst, A. (2017). MLKL Activation Triggers NLRP3-Mediated Processing and Release of IL-1β Independently of Gasdermin-D. J. Immunol*. 198,* 2156-2164.

Halle, A., Hornung, V., Petzold, G., Stewart, C.R., Monks, B.G., Reinheckel, T., Fitzgerald, K.A., Latz, E., Moore, K.J., and Golenbock, D.T. (2008) The NALP3 inflammasome is involved in the innate immune response to amyloid-β. Nat. Immunol. 9, 857–865.

Harder, J., Franchi, L., Muñoz-Planillo, R., Park, J-H., Reimer, T., and Núñez, G. (2009). Activation of the Nlrp3 Inflammasome by Streptococcus pyogenes Requires Streptolysin O and NF-κB Activation but Proceeds Independently of TLR Signaling and P2X7 Receptor. J. Immunol. *183*, 5823-5829.

He, W-T., Wan, H., Hu, L., Chen, P., Wang, X., Huang, Z., Yang, Z-H., Zhong, C-Q., and Han, J. (2015). Gasdermin D is an executor of pyroptosis and required for interleukin-1β secretion. Cell Res. *25,* 1285–1298.

He, Y., Zeng, M. Y., Yang, D., Motro, B., and Nunez, G. (2016). NEK7 is an essential mediator of NLRP3 activation downstream of potassium efflux. Nature *530*, 354+.

Horner, S.M., Liu, H.M., Park, H.S., Briley, J., and Gale, Jr., M. (2011). Mitochondrial-associated endoplasmic reticulum membranes (MAM) form innate immune synapses and are targeted by hepatitis C virus. Proc. Natl. Acad. Sci. USA *108*, 14590-14595.

Horner, S.M., Wilkins, C., Badil, S., Iskarpatyoti, J., and Gale Jr., M. (2015). Proteomic Analysis of Mitochondrial-Associated ER Membranes (MAM) during RNA Virus Infection Reveals Dynamic Changes in Protein and Organelle Trafficking. PLoS ONE *10*, e0117963.

Horng, T. (2014). Calcium signaling and mitochondrial destabilization in the triggering of the NLRP3 inflammasome. Trends Immunol. *35*, 253-261.

Hornung, V., Bauernfeind, F.,Halle, A.,Samstad, E.O., Kono, H., Rock, K.L., Fitzgerald, K.A., and Latz, E. (2008). Silica crystals and aluminum salts activate the NALP3 inflammasome through phagosomal destabilization. Nat. Immun. *9*, 847-856.

Ichinohe, T., Yamazaki, T., Koshiba, T., and Yanagi, Y. (2013). Mitochondrial protein mitofusin 2 is required for NLRP3 inflammasome activation after RNA virus infection. Proc. Natl. Acad. Sci. USA *110*, 17963-17968.

Iyer, S.S., He, Q., Janczy, J.R., Elliott, E.I., Zhong, Z., Olivier, A.K., Sadler, J.J., Knepper-Adrian, V., Han, R., Qiao, L., et al. (2013). Mitochondrial cardiolipin is required for Nlrp3 inflammasome activation. Immunity *39*, 311-23.

Jorgensen, I. and Miao, E.A. (2015). Pyroptotic cell death defends against intracellular pathogens. Immunol. Rev. *265*, 130-142.

Kanneganti, T-D. (2010). Central roles of NLRs and inflammasomes in viral infection. Nat. Rev. Immunol. *10*, 688-698.

Kaplan, R.S., Mayor, J.A., and Wood, D.O. (1993). The mitochondrial tricarboxylate transport protein. cDNA cloning, primary structure, and comparison with other mitochondrial transport proteins. J. Biol. Chem. *268,* 13682-13690.

Kato, T., Date, T., Murayama, A., Morikawa, K., Akazawa, D., and Wakita, T. (2006). Cell culture and infection system for hepatitis C virus. Nat. Protoc. *1,* 2334-2339.

Katsnelson, M. A., Rucker, L. G., Russo, H. M., and Dubyak, G. R. (2015). K^+ Efflux Agonists Induce NLRP3 Inflammasome Activation Independently of Ca^{2+} Signaling. J. Immunol. *194,* 3937-3952.

Katsnelson, M.A., Lozada-Soto, K. M., Russo, H. M., Miller, B. A., and Dubyak, G. R. (2016). NLRP3 inflammasome signaling is activated by low-level lysosome disruption but inhibited by extensive lysosome disruption: roles for K^+ efflux and Ca^{2+} influx. Am. J. Physiol. - Cell Physiol. *311*, C83–C100.

Kim S-M, Kim Y.G, Kim D-J, Park S.H, Jeong K-H, Lee Y.H, Lim S.J, Lee S-H, and Moon J-Y. (2018). Inflammasome-Independent Role of NLRP3 Mediates Mitochondrial Regulation in Renal Injury. Front. Immunol. *9,* 2563.

Kovacs, S.B. and Miao, E.A. (2017). Gasdermins: Effectors of Pyroptosis. Trends Cell Biol. *27,* 673-684.

Lamkanfi, M., Kalai, M., Saelens, X., Declercq, W., and Vandenabeele, P. (2004) Caspase-1 Activates Nuclear Factor of the kappa-Enhancer in B Cells Independently of Its Enzymatic Activity. J. Biol. Chem. *279*, 24785–24793.

Lamkanfi, M. and Dixit, V.M. (2012). Inflammasomes and Their Roles in Health and Disease. Ann. Rev. Cell Dev. Biol. *28*, 137-161.

Latz, E., Xiao, T.S., and Stutz, A. (2013). Activation and regulation of the inflammasomes. Nat. Rev. Immunol. *13*, 397-411.

Lee, G-S., Subramanian, N., Kim, A.I., Aksentijevich, I., Goldbach-Mansky, R., Sacks, D.B., Germain, R.N., Kastner, D.L., and Chae, J.J. (2012). The calcium-sensing receptor regulates the NLRP3 inflammasome through Ca^{2+} and cAMP. Nature *492,* 123–127.

Li, X., Thome, S., Ma, X., Amrute-Nayak, M., Finigan, A., Kitt, L., Masters, L., James, J. R., Shi, Y., Meng, G, et al. (2017). MARK4 regulates NLRP3 positioning and inflammasome activation through a microtubule-dependent mechanism. Nat. Commun. *8,* 15986.

Liu, Q., Zhang, D., Hu, D., Zhou, X., and Zhou, Y. (2018). The role of mitochondria in NLRP3 inflammasome activation. Mol. Immunol. *103*, 115–124.

Liu, X., Zhang, Z., Ruan, J., Pan, Y., Magupalli, V.G., Wu, H., and Lieberman, J. (2016). Inflammasome-activated gasdermin D causes pyroptosis by forming membrane pores. Nature *535*, 153-158.

Lupfer, C., Malik, A., and Kanneganti, T-D. (2015). Inflammasome control of viral infection. Curr. Opinion in Vir. *12*, 38–46.

Mariathasan, S., Weiss, D.S., Newton, K., McBride, J., O'Rourke, K., Roose-Girma, M., Lee, W.P., Weinrauch, Y., Monack, D.M., and Dixit, V.M. (2006). Cryopyrin activates the inflammasome in response to toxins and ATP. Nature *440*, 228-232.

Marmol, P., Pardo, B., Wiederkehr, A., del Arco, A., Wollheim, C.B., and Satrustegui, J. (2009). Requirement for Aralar and Its Ca2+-binding Sites in Ca2+ Signal Transduction in Mitochondria from INS-1 Clonal beta-Cells. J. Biol. Chem. *284,* 515-524.

Martinon, F., Petrilli, V., Mayor, A., Tardivel, A., and Tschopp, J. (2006). Gout-associated uric acid crystals activate the NALP3 inflammasome. Nature *440*, 237-241.

Mayor, A., Martinon, F., De Smedt, T., Pétrilli, V., and Tschopp, J. (2007). A crucial function of SGT1 and HSP90 in inflammasome activity links mammalian and plant innate immune responses. Nat. Immunol. *8*, 497-503.

McWhirter, S.M., tenOever, B.R., and Maniatis, T. (2005). Connecting Mitochondria and Innate Immunity. Cell *122,* 645-647.

Medzhitov, R. (2008). Origin and physiological roles of inflammation. Nature *454*, 428–435.

Mellacheruvu, D., Wright, Z., and Nesvizhskii, A.I. (2013). The CRAPome: a contaminant repository for affinity purification–mass spectrometry data. Nat. Methods *10,* 730–736. https://reprint-apms.org/

Misawa, T., Takahama, M., Kozaki, T., Lee, H., Zou, J., Saitoh, T., and Akira, S. (2013). Microtubule-driven spatial arrangement of mitochondria promotes activation of the NLRP3 inflammasome. Nat. Immunol. *14*, 454–460.

Missiroli, S., Patergnani, S., Caroccia, N., Pedriali, G., Perrone, M., Previati, M., Wieckowski, M.R., Giorgi, C. (2018). Mitochondria-associated membranes (MAMs) and inflammation. Cell Death Dis. *9*, 329.

Monteleone, M., Stanley, A.C., Chen, K.W., Brown, D.L., Bezbradica, J.S., von Pein, J.B., Holley, C.L., Boucher, D., Shakespear, M.R., Kapetanovic, R., et al. (2018). Interleukin-1β Maturation Triggers Its Relocation to the Plasma Membrane for Gasdermin-D-Dependent and -Independent Secretion. Cell Reports *24,* 1425-1433.

Moon, J-S., Lee, S., Park, M-A., Siempos, I.I., Haslip, M., Lee, P.J., Yun, M., Kim, C.K., Howrylak, J., Ryter, S.W., et al. (2015). UCP2-induced fatty acid synthase promotes NLRP3 inflammasome activation during sepsis. J. Clin. Invest. *125,* 665–680.

Mosaoa, R., Kasprzyk-Pawelec, A., Fernandez, H.R., and Avantaggiati, M.L. (2021). The Mitochondrial Citrate Carrier SLC25A1/CIC and the Fundamental Role of Citrate in Cancer, Inflammation and Beyond. Biomolecules 11(2), 141.

Muñoz-Planillo, R., Kuffa, P., Martinez-Colon, G., Smith, B.L., Rajendiran, T.M., and Nuñez, G. (2013). K^+ Efflux Is the Common Trigger of NLRP3 Inflammasome Activation by Bacterial Toxins and Particulate Matter. Immunity *38*, 1142-1153.

Murakami, T., Ockinger, J., Yu, J., Byles, V., McColl, A., Hofer, A.M., and Horng, T. (2012). Critical role for calcium mobilization in activation of the NLRP3 inflammasome. Proc. Natl. Acad. Sci. USA *109*, 11282-11287.

Negash, A.A., Ramos, H.J., Crochet, N., Lau, D.T.Y., Doehle, B., Papic, N., Delker, D.A, Jo, J., Bertoletti, A., Hagedorn, C.H., and Gale Jr., M. (2013). IL-1β Production through the NLRP3 Inflammasome by Hepatic Macrophages Links Hepatitis C Virus Infection with Liver Inflammation and Disease. PLoS Path. *9*, e1003330.

Orlowski, G.M., Colbert, J.D., Sharma, S., Bogyo, M., Robertson, S.A., and Rock, K.L. (2015). Multiple Cathepsins Promote Pro–IL-1β Synthesis and NLRP3-Mediated IL-1β Activation. J. Immunol. *195*, 1685-1697.

Palmieri, F. (2013). The mitochondrial transporter family SLC25: identification, properties and physiopathology. Mol. Aspects Med. *34*, 465-484.

Palmieri, F. (2014). Mitochondrial transporters of the SLC25 family and associated diseases: a review. J. Inherit. Metab. Dis. *37,* 565-575.

Palmieri, F. and Monné, M. (2016). Discoveries, metabolic roles and diseases of mitochondrial carriers: A review. Biochimica et Biophysica Acta – Mol. Cell Res. *1863,* 2362-2378.

Palmieri, L., Pardo, B., Lasorsa, F.M., del Arco, A., Kobayashi, K., Iijima, M., Runswick, M.J., Walker, J.E., Saheki, T., Satrustegui, J., et al. (2001). Citrin and aralar1 are Ca^{2+}-stimulated aspartate/glutamate transporters in mitochondria. EMBO J. *20*, 5060-5069.

Park, S., Park, S., Juliana, C., Hong, S., Datta, P., Hwang, I., Fernandes-Alnemri, T., Yu, J.-W. and Alnemri, E.S. (2013). The mitochondrial antiviral protein MAVS associates with NLRP3 and regulates its inflammasome activity. J. Immunol. *191*, 4358-4366.

Pazár, B., Ea, H.K., Narayan, S., Kolly, L., Bagnoud, N., Chobaz, V., Roger, T., Liote´, F., So, A., and Busso, B. (2011). Basic Calcium Phosphate Crystals Induce Monocyte/Macrophage IL-1β Secretion through the NLRP3 Inflammasome In Vitro. J. Immunol. *186*, 2495-2502.

Pétrilli, V., Papin, S., Dostert, C., Mayor, A., Martinon, F., and Tschopp, J.(2007). Activation of the NALP3 inflammasome is triggered by low intracellular potassium concentration. Cell Death Differ. *14*, 1583–1589.

Pflugheber, J., Fredericksen, B., Sumpter Jr., R., Wang, C., Ware, F., Sodora, D.L., and Gale Jr., M. (2002). Regulation of PKR and IRF-1 during hepatitis C virus RNA replication. Proc. Natl. Acad. Sci. USA *99,* 4650-4655.

Prochnicki, T. and Latz, E. (2017). Inflammasomes on the Crossroads of Innate Immune Recognition and Metabolic Control. Cell Metab. *26,* 71-93.

Py, B.F., Kim, M-S., Vakifahmetoglu-Norberg, H., and Yuan, J. (2013). Deubiquitination of NLRP3 by BRCC3 Critically Regulates Inflammasome Activity. Mol. Cell. *49,* 331–338.

Rajanbabu, V., Galam, L., Fukumoto, J., Enciso, J., Tadikonda, P., Lane, T.N., Sayantani Bandyopadhyay, S., Parthasarathy, P.T., Cho, Y., et al. (2015). Genipin suppresses NLRP3 inflammasome activation through uncoupling protein-2. Cellular Immunol. *297*, 40-45.

Rao, Z., Chen, X., Wu, J., Xiao, M., Zhang, J., Wang, B., Fang, L., Zhang, H., Wang, X., Yang, S., et al. (2019). Vitamin D Receptor Inhibits NLRP3 Activation by Impeding Its BRCC3-Mediated Deubiquitination. Front. Immunol. *10*, 2783.

Rathinam, V.A.K., Jiang, Z., Waggoner, S.N., Sharma, S., Cole, L.E., Waggoner, L., Vanaja, S. K., Monks, B.G., Ganesan, S., Latz, E., et al. (2010). The AIM2 inflammasome is essential for host defense against cytosolic bacteria and DNA viruses. Nat. Immunol. *11*, 395–402.

Robinson, K. S., Teo, D.E.T., Tan, K.S., Toh, G.A., Ong, H.H., Lim, C.K., Lay, K., Au, B.V., Lew, T.S., Chu, J.J. H., et al. (2020). Enteroviral 3C protease activates the human NLRP1 inflammasome in airway epithelia. Science *370,* eaay 2002.

Ruprecht, J.J., and Kunji, E.R.S. (2019). The SLC25 Mitochondrial Carrier Family: Structure and Mechanism. Trends Biochem. Sci. *45,* 244-258.

Saheki, T. and Kobayashi, K. (2002). Mitochondrial aspartate glutamate carrier (citrin) deficiency as the cause of adult-onset type II citrullinemia (CTLN2) and idiopathic neonatal hepatitis (NICCD). J. Hum. Genet. *47*, 333-341.

Saheki, T., Iijima, M., Li, M.X., Kobayashi, K., Horiuchi, M., Ushikai, M., Okumura, F., Meng, X.J., Inoue, I., Tajima, et al. (2007). Citrin/Mitochondrial Glycerol-3-phosphate Dehydrogenase Double Knock-out Mice Recapitulate Features of Human Citrin Deficiency. J. Biol. Chem. *282,* 25041-25052.

Sanders, A.A.W.M. and Kaverina, I. (2015). Nucleation and Dynamics of Golgi-derived Microtubules. Front. Neurosci. *9,* 431.

Sandstrom, A., Mitchell, P.S., Goers, L., Mu, E.W., Lesser, C. F., and Vance, R. E. (2019). Functional degradation: A mechanism of NLRP1 inflammasome activation by diverse pathogen enzymes. Science *364*, eaau 1330.

Sanman, L.E., Qian, Y., Eisele, N.A., Ng, T.M., van der Linden, W.A., Monack, D.M., Weerapana, E., and Bogyo, M. (2016). Disruption of glycolytic flux is a signal for inflammasome signaling and pyroptotic cell death. eLife *5*, e13663.

Schnappauf, O., Chae, J.J., Kastner, D.L., and Aksentijevich, I. (2019). The Pyrin Inflammasome in Health and Disease. Front. Immunol. *10*, 1745.

Schroder, K. and Tschopp, J. (2010). The Inflammasomes. Cell *140*, 821–832.

Seok, J.K., Kang, H.C., Cho, Y-Y., Lee, H.S., and Lee, J.Y. (2021). Regulation of the NLRP3 Inflammasome by Post-Translational Modifications and Small Molecules. Front. Immunol. *11*, 618231.

Sharif, H., Wang, L., Wang, W.L., Magupalli, V.G., Andreeva, L., Qiao, Q., Hauenstein, A.V., Wu, Z., Núñez, G., Mao, Y., et al. (2019). Structural mechanism for NEK7-licensed activation of NLRP3 inflammasome. Nature *570*, 338-343.

Shi, H., Wang, Y., Li, X., Zhan, X., Tang, M., Fina, M., Su, L., Pratt, D., Bu, C. H., Hildebrand, S., et al. (2016). NLRP3 activation and mitosis are mutually exclusive events coordinated by NEK7, a new inflammasome component. Nat. Immunol. *17,* 250–258.

Shi, J., Zhao, Y., Wang, K., Shi, X., Wang, Y., Huang, H., Zhuang, Y., Cai, T., Wang, F., and Shao, F. (2015). Cleavage of GSDMD by inflammatory caspases determines pyroptotic cell death. Nature *526*, 660–665.

Shimada, K., Crother, T.R., Karlin, J., Dagvadorj, J., Chiba, N., Chen, S., Ramanujan, V.K., Wolf, A.J., Vergnes, L., Ojcius, D.M., et al. (2012). Oxidized Mitochondrial DNA Activates the NLRP3 Inflammasome during Apoptosis. Immunity *36*, 401-414.

Sinasac, D.S., Moriyama, M., Jalil, M.A., Begum, L., Li, M.X., Iijima, M., Horiuchi, M., Robinson, B.H., Kobayashi, K., Saheki, T., et al. (2004). Slc25a13-knockout mice harbor metabolic deficits but fail to display hallmarks of adult-onset type II citrullinemia. Mol. Cell Biol. *24,* 527-536.

Song, H., Liu, B., Huai, W., Yu, Z., Wang, W., Zhao, J., Han, L., Jiang, G., Zhang, L., Gao, C, et al. (2016). The E3 ubiquitin ligase TRIM31 attenuates NLRP3 inflammasome activation by promoting proteasomal degradation of NLRP3. Nat. Commun. *7,* 13727.

Spalinger, M.R., Kasper, S., Gottier, C., Lang, S., Atrott, K., Vavricka, S.R., Scharl, S., Gutte, P.M., Grütter, M.G., Beer, H-D., et al. (2016). NLRP3 tyrosine phosphorylation is controlled by protein tyrosine phosphatase PTPN22. J. Clin. Invest. *126*, 1783-1800.

Strowig, T., Henao-Mejia, J., Elinav, E., and Flavell, R. (2012). Inflammasomes in health and disease. Nature *481,* 278-286.

Subramanian, N., Natarajan, K., Clatworthy, M.R., Wang, Z., and Germain, R.N. (2013). The adaptor MAVS promotes NLRP3 mitochondrial localization and inflammasome activation. Cell *153*, 348-361.

Sutterwala, F.S., Haasken, S., Cassel, S.L. (2014). Mechanism of NLRP3 inflammasome activation. Ann. NY Acad. Sci. *1319*, 82-95.

Swanson, K.V., Deng, M., and Ting, J.P-Y. (2019). The NLRP3 inflammasome: molecular activation and regulation to therapeutics. Nat. Rev. Immun. *19*, 477-489.

Szymanski, J., Janikiewicz, J., Michalska, B., Patalas-Krawczyk, P., Perrone, M., 2, Ziółkowski, W., Duszynski, J., Pinton, P., Dobrzyn, A., and Wieckowski, M.R. (2017). Review: Interaction of Mitochondria with the Endoplasmic Reticulum and Plasma Membrane in Calcium Homeostasis, Lipid Trafficking and Mitochondrial Structure. Int. J. Mol. Sci. *18*, 1576.

Tannahill, G., Curtis, A., Adamik, J. et al. (2013). Succinate is an inflammatory signal that induces IL-1β through HIF-1α. Nature *496,* 238–242.

Thangaratnarajah, C., Ruprecht, J.J., and Kunji, E.R.S. (2014). Calcium-induced conformational changes of the regulatory domain of human mitochondrial aspartate/glutamate carriers. Nat. Comm. *5*, 5491.

The ORFeome Collaboration., Wiemann, S., Pennacchio, C. et al. (2016). The ORFeome Collaboration: a genome-scale human ORF-clone resource. Nat. Methods *13,* 191–192.

van der Burgh, R., Nijhuis, L., Pervolaraki, K., Compeer, E.B., Jongeneel, L.H., van Gijn, M., Coffer, P.J., Murphy, M.P., Mastroberardino, P.G., Frenkel, J., et al. (2014). Defects in Mitochondrial Clearance Predispose Human Monocytes to Interleukin-1β Hypersecretion. J. Biol. Chem. *289*, 5000-5012.

Vozza, A., Parisi, G., De Leonardis, F., Lasorsa, F.M., Castegna, A., Amorese, D., Marmo, R., Calcagnile, V.M., Palmieri, L., Ricquier, D., et al. (2014). UCP2 transports C4 metabolites out of mitochondria, regulating glucose and glutamine oxidation. Proc. Natl. Acad. Sci. USA *111*, 960-965.

Weinberg, S.E., Sena, L.A., and Chandel, N.S. (2015). Mitochondria in the Regulation of Innate and Adaptive Immunity. Immunity *42,* 406-417.

Wibom, R., Lasorsa,F.M., Töhönen, V., Barbaro, M., Sterky, F.H., Kucinski, T., Naess, K., Jonsson, M., Pierri, C.L., Palmieri, F., et al. (2009). AGC1 Deficiency Associated with Global Cerebral Hypomyelination. New Engl. J. Med. *361*, 489-495.

Wolf, A.J., Reyes, C.N., Liang, W., Becker, C., Shimada, K., Wheeler, M.L., Cho, H.C., Popescu, N.I., Coggeshall, K.M., Arditi, M., and Underhill, D.M. (2016). Hexokinase Is an Innate Immune Receptor for the Detection of Bacterial Peptidoglycan. Cell *166,* 624–636.

Yang, J., Zhao, Y., Shi, J., and Shao, F. (2013). Human NAIP and mouse NAIP1 recognize bacterial type III secretion needle protein for inflammasome activation. Proc. Natl. Acad. Sci. USA *110,* 14408-14413.

Yasukawa, K., Kinoshita, D., Yaku, K., Nakagawa, T., and Koshiba, T. (2020). The microRNAs miR-302b and miR-372 regulate mitochondrial metabolism via the SLC25A12 transporter, which controls MAVS-mediated antiviral innate immunity. J. Biol. Chem. *295,* 444-457.

Yu, P., Zhang, X., Liu, N. Tang, L., and Peng, C. (2021). Pyroptosis: mechanisms and diseases. Sig. Transduct. Target Ther. *6*, 128.

Zhang, Z., Meszaros, G., He, W.-t., Xu, Y., Magliarelli, H.d.F., Mailly, L., Mihlan, M., Liu, Y., Gámez, M.P., Goginashvili, A., et al. (2017). Protein kinase D at the Golgi controls NLRP3 inflammasome activation. J. Exp. Med. *214*, 2671–2693.

Zhao, Y., Yang, J., Shi, J., Gong, Y-N., Lu, Q., Xu, H., Liu,. L., and Shao, F. (2011). The NLRC4 inflammasome receptors for bacterial flagellin and type III secretion apparatus. Nature *477*, 596–600.

Zhong, Z., Liang, S., Sanchez-Lopez, E., He, F., Shalapour, S., Lin, X., Wong, J., Ding, S., Seki, E., Schnabl, B., et al. (2018). New mitochondrial DNA synthesis enables NLRP3 inflammasome activation. Nature *560,* 198–203.

Zhou, R., Yazdi, A.S., Menu, P., and Tschopp, J. (2011). A role for mitochondria in NLRP3 inflammasome activation. Nature *469*, 221-225.